Photocopy and Use Authorization

In presenting this thesis in partial fulfillment of the requirements for an advanced degree at Idaho State University, I agree that the Library shall make it freely available for inspection. I further state that permission for extensive copying of my thesis for scholarly purposes may be granted by the Dean of the Graduate School, Dean of my academic division, or by the University Librarian. It is understood that any copying or publication of this thesis for financial gain shall not be allowed without my written permission.

Signature: ____

Date: ______________________________

Land Cover Change and Habitat Monitoring of Columbian Sharp-tailed Grouse in Southeast Idaho

by

Thomas Calton

A thesis

submitted in partial fulfillment

of the requirements for the degree of

Master of Science in Geographic Information Science

Idaho State University

Fall 2019

Committee Approval

To the Graduate Faculty:

The members of the committee appointed to examine the thesis of THOMAS CALTON find it satisfactory and recommend that it be accepted.

Dr. Donna Delparte,
Associate Professor, Department of Geosciences,
College of Science and Engineering
Idaho State University
Major Advisor

Dr. Carrie Bottenberg,
Assistant Professor, Department of Geosciences,
College of Science and Engineering
Idaho State University
Committee Member

Dr. Charles Petersen
Professor, Department of Biological Sciences
College of Science and Engineering
Idaho State University
Graduate Faculty Representative

Dedication

For my dear wife, without whom I would not be able to get through much of anything, much less a master's thesis.

For my dear children, whom all this work is truly for. If you never realize what we have been through to give you the lives you deserve…. good.

For the rest of my family, that still has no clue what it is that I actually do but are supportive and nod their heads like they understand what LiDAR and photogrammetry are.

Acknowledgements

I would like to thank all those who have helped me along the way and made it possible for me to accomplish this work. To Dr. Donna Delparte, for being a great major advisor and boss for the last few years, and for providing just enough days at just the right times to get out and fly. Dr. H. Carrie Bottenberg for providing a sounding board for ideas and for being a great instructor and teacher of many things I only thought I knew. To the rest of the instructors and staff in the ISU Geosciences department for the support and handling of just about anything administrative so I did not have to.

To my fellow graduate and undergraduate students who helped make this happen: co-pilots Dusten Lish, Sarah Tetzlof, Dalton Blocker, Selena Barrett, and Dane Lubenow, for helping me keep the bird in the air and collecting all the data. To the same group, plus Emma Thackray, for setting ground control points and Dusten for assisting me with the vegetation inventory of all those points.

I would like to acknowledge Idaho Fish and Game for their funding support and mentorship. To Matt Pieron for getting all this started for me, Scott Bergen, Shane Roberts and Zach Lockyer for spending time with me to fine tune the focus of the research. I hope that my work and findings can support future work as the project continues to develop.

This thesis is also supported by "RII Track-1: Linking Genome to Phenome to Predict Adaptive Responses of Organisms to Changing Landscapes," funded under the National Science Foundation grant No. OIA-1757324. Any opinions, findings, and conclusions or recommendations expressed in this material are those of the author and do not necessarily reflect the views of the National Science Foundation.

Table of Contents

List of Figures

List of Tables

List of Abbreviations

COTS	Commercial Off the Shelf
CSTG	Columbian Sharp-tailed Grouse
CRP	Conservation Reserve Program
Esri	Environmental Systems Research Institute
FWHM	Full Width at Half Maximum
GCP	Ground Control Point
GNSS	Global Navigation Satellite System
GPS	Global Positioning System
GWR	Geographically Weighted Regression
HSI	HyperSpectral Imager
IDFG	Idaho Department of Fish and Game
LAI	Leaf Area Index
NDVI	Normalized Difference Vegetation Index
NLCD	National Land Cover Dataset
sUAS	Small Unmanned Aerial System
UgCS	Universal Ground Control Software
VI	Vegetation Indices

Land Cover Change and Habitat Monitoring of Columbian Sharp-tailed Grouse in Southeast Idaho

Thesis Abstract – Idaho State University (2019)

Anthropogenic forces of land use and land cover change have affected Columbian Sharp-tailed grouse habitats in southeastern Idaho over the past century, with the assumption that the decline in bird counts at lek sites relates to the increase and distribution of agricultural operations. This study performed an analysis of areas surrounding lek locations to highlight the effect that land management practices have on grouse habitat. This work examines land cover change between 2001 and 2016 using the National Land Cover Dataset to evaluate the relationship between the change in bird counts at 69 lek sites and the reduction in habitat. For the time period there was a 5.8% change to agriculture resulting in no significant correlation between lek count numbers and land cover change. Small unmanned aerial systems (sUAS) equipped with hyperspectral sensors were deployed to map and classify the vegetative composition, resulting in high resolution habitat maps.

Key Words: Columbian Sharp-tailed Grouse, habitat mapping, sUAS, hyperspectral, photogrammetry, remote sensing, Conservation Reserve Program

Chapter 1 Introduction

1.1 Introduction

Columbian Sharp-tailed Grouse (*Tympanuchus phasianellus columbianus,* CSTG) populations have been in decline, initially, because of overhunting in the mid to late 19th century and subsequently because of land conversion since the turn of the 20th century (Buss & Dziedzic, 1955; Connelly, Schroeder, Sands, & Braun, 2000; McDonald & Reese, 1998). CSTG are a species of gallinaceous upland game bird (Andersen et al., 2015). Formerly, CSTG occupied a range from central British Columbia to California and Colorado (Marks & Marks, 1988). Currently, CSTG only occupy small areas within British Columbia, southeast Idaho, south-central Wyoming, northern Utah, and northwestern Colorado. Historically, the habitats of CSTG were dominated by grasslands consisting of bunch grasses and sagebrush steppe (McDonald & Reese, 1998). Early 20th century settlement of CSTG home range resulted in greater mechanization of farming practices and an increase of cultivated acres (Buss & Dziedzic, 1955). Intensive cultivation practices led to greater fragmentation of natural CSTG habitats. Habitat fragmentation has resulted in fewer CSTG populations that encompass multiple lek locations (McDonald & Reese, 1998). A lek is a traditional dancing ground where male birds of the species congregate to display for reproductive purposes (Leupin, 2003). Excessive livestock grazing, overuse of herbicides, and burning of stubble fields has also had a negative impact on CSTG numbers (Giesen & Connelly, 1993). Idaho supports approximately 60-65% of the remaining CSTG in the U.S, and is home to one of three populations that make up 95% of remaining breeding populations (Andersen et al., 2015).

CSTG rely on a diversity of vegetation communities for all life stages. Female nest site selection is dependent on available vegetation and corresponds to sites with a dense shrub cover of species such as rabbit brush (*Ericameria spp*.) and sage (*Artemisia spp*.) for nesting success (Giesen & Connelly, 1993). For brooding, CSTG typically select areas with lower brush density that are dominated by species such as snowberry (*Symphoricarpos albus*) and sage (*Artemisia spp.*) (Klott & Lindzey, 1990). Male CSTG generally select lek sites located on knolls or ridgetops that are characterized by a high abundance of native bunch grasses such as Idaho Fescue (*Festuca idahoensis*), Mountain Brome (*Bromus marginatus*), and Snake River Wheatgrass (*Elymus wawawaiensis*), and typically include a much higher brushy component than sites selected by other sub-species of sharp-tailed grouse like plains sharp-tailed grouse *(P. t. jamesi)* and prairie sharp-tailed grouse *(P. t. campestris)* (Giesen & Connelly, 1993). There is limited evidence that dense cover on leks is detrimental to reproduction and survival of CSTG, but Klott & Lindzey (1990) reported less vegetative cover on lek sites than random sites.

Small Unmanned Aerial Systems (sUAS) are improving the ability to capture high spatial resolution data concerning wildlife habitats at a relatively inexpensive cost (Gonzalez et al., 2016). Recent developments in sUAS technologies and relaxing operational regulations present new opportunities for environmental monitoring (Linchant, Lisein, Semeki, Lejeune, & Vermeulen, 2015). sUAS offers another level of hierarchal sampling; they provide visual imagery at a localized and a biologically distinguishable level (Jones, Pearlstine, & Percival, 2006). Because of the key advantages of high resolution and opportunities to fly more frequently, sUAS offers greater temporal and spectral resolution when fitted with multispectral or hyperspectral sensors. Experiments have demonstrated that sUAS are capable of delivering georeferenced maps of biochemical and biophysical variables of vegetation at sub five centimeter resolution (Lucieer, Malenovský, Veness, & Wallace, 2014).

Management decisions about habitat restoration demands an increasing level of accurate and precise data. As funds for habitat conservation are limited, it is imperative to employ cost effective and time saving methods for data collection, while at the same time increasing the amount of data available to researchers and managers so they can make the best possible decisions. This study aims to complete two major objectives: 1) Examine the relationship between land cover change and the number of CSTG that visit lek sites across southeast Idaho, and 2) determine the fine scale vegetation composition of brooding and nesting sites for CSTG as classified using a hyperspectral imager mounted on a sUAS. By generating vegetation models from sUAS flights, this project maps vegetative composition within 4 km of five lek locations found in southeastern Idaho.

1.2 Study Area

The study area for this project encompasses southeast Idaho. The focus is on Bannock, Oneida and Power counties, with attention given to Marsh, Arbon, Rockland and Malad valleys along with the area surrounding the community of Holbrook (Figure 1). The habitats in this study area receive 30-50 cm of rain annually. Upland habitats range from low to mid valley elevations, with moderately rolling terrain. Objective one includes the entirety of this area, using 2001 and 2016 land cover datasets from the Multi-Resolution Land Characteristics (MRLC) Consortium's National Land Cover Dataset (NLCD). Yellow points on the map indicate all documented leks (317) within the three-county area. Blue dots indicate lek sites (69) used in chapter 3 for analysis with land cover change. The

Idaho Department of Fish and Game (IDFG) conduct yearly bird counts at lek sites across southeast Idaho. Bird counts occur in the spring when male CSTG are displaying at leks for reproductive purposes. The counts are the main indicator of the trend within CSTG populations. Not all leks are counted every year due to staffing limitations. Out of the 870 leks in the entire state, an average of about 200 have been counted every year for the last decade (2009-2018). Objective two focuses on a small area (388.5 ha), flown with a sUAS, located northeast of Downey, ID.

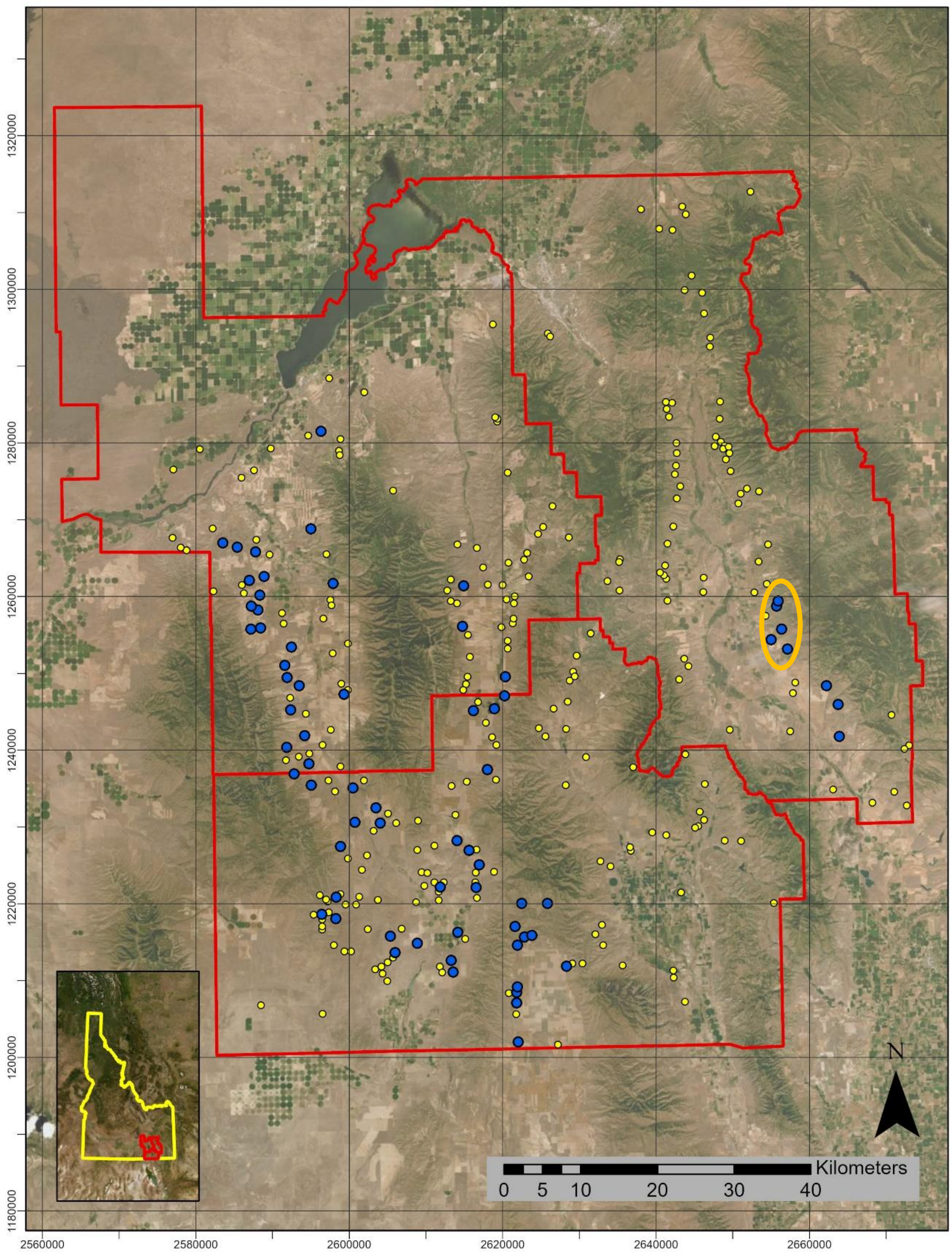

Figure 1. Study Area in southeast Idaho. Yellow dots are all 317 historical lek sites within Bannock, Oneida, and Power counties. Blue dots represent lek locations used in chapter 3 analysis. Area indicated by yellow ellipse is the study area for chapter 4.

1.3 Broader Impacts

One of the aims of this research is to identify areas influenced by high levels of land cover change at a regional scale. Understanding land use conversion, and its effect on CTSG, at regional and landscape scales is paramount to informing management decisions and planning future rehabilitation efforts. The successful application of this knowledge will lead to the development of cost-effective ways to target conservation measures. Further, by introducing the use of sUAS for mapping fine scale vegetation composition, this innovative approach explores the functionality of this technology for agencies wanting to develop a greater understanding of CSTG habitat requirements. We are providing our collaborative partner, Idaho Fish and Game, with the outcomes from this study.

This project contributes to the research efforts of the Idaho EPSCoR, GEM3, Genes by Environment program (NSF Award No. OIA-1757324). Mapping land cover change in southeast Idaho and developing fine scale habitat maps supplies a foundation of data to the GEM3 mapping team to examine the spatiotemporal links between genomic diversity, phenotypic plasticity, and social ecological systems change. Further, the GEM3 team will teach workflows to plan and conduct sUAS flights and steps to process and analyze imaged hyperspectral data in Vertically Integrated Projects (VIP). VIP courses at Idaho institutions provide research-based educational opportunities to a diverse student body, covering both undergraduate and graduate levels in a range of disciplines including biological and natural sciences, engineering, and social sciences. This strategy offers students at all levels to benefit from this work through the development of lab modules, research opportunities, and mentoring from faculty and staff. It also supports workforce development and professional training through interdisciplinary team collaboration, mentor training, and career mapping.

Chapter 2 Literature Review

2.1 Columbian Sharp-tailed Grouse Range and Habitat Requirements

Columbian Sharp-tailed Grouse (CSTG) is a lekking species of bird. A lek is an area in which male birds congregate to perform courtship displays to compete for females and the opportunity to mate. Giesen and Connelly (1993) stated that leks are established in grassy or weedy areas of shrub-land. These leks are usually 30 m in diameter, and are typically found in close proximity to suitable nesting and brood-rearing cover (Andersen et al., 2015). There is some consensus as to the distance from a lek that female CSTG will nest. Typically, females nest in areas that are within 2 km of the lek location (Andersen et al., 2015; Boisvert, Hoffman, & Reese, 2005; Leupin, 2003). Boisevert et al. (2005) found that 85% percent of females studied nested within 2 km of the lek. Leupin (2003) found that the largest proportion of females located in British Columbia, nest within 2.4 km of the lek. Geisen & Connelly (1993) state a shorter distance of less than 1.6 km, but they conceded that nests have been located at distances greater than 3 km from the lek site.

Winter habitat range differs from nesting and brooding habitats. Boisevert et al. (2005) found that 100% of the birds they studied wintered at distances greater than 3 km from the lek site at which they were captured. Andersen et al. (2015) stated that Sharp-tailed grouse travel anywhere from 0.5 km to greater than 40 km for wintering habitat. Giesen and Connelly (1993) noted that birds travel anywhere from 2.6 km to 4.5 km with some outliers travelling as much as 20 km to wintering habitats in regions that are lacking a broad distribution of winter food resources compared to regions where resources are plentiful. CSTG rely on deciduous trees and shrubs for their winter habitat. Marks & Marks (1988) found that Sharp-tailed grouse fed primarily on hawthorn (*Crataegus douglasii*) fruits and on serviceberry (*Amelanchier alnifolia*) and chokecherry (*Prunus virginiana)* buds, when snow covered the ground. Leupin (2003) classified winter habitats dominated by quaking aspen (*Populus tremuloides*), Douglas fir (*Pseudotsuga menziesii*), mountain snowberry (*Symphoricarpos oreophilus*), prickly rose (*Rosa acicularis*), and red-osier dogwood (*Cornus sericea*). The consensus is that Sharp-tailed grouse rely on a brushy cover type habitat that includes a large number of fruiting bushes for all life stages, but most importantly in winter (Andersen et al., 2015; Boisvert et al., 2005; Giesen & Connelly, 1993; Leupin, 2003; Marks & Marks, 1988).

Columbian Sharp-tailed grouse have declined in western North America since the beginning of the 20th century (Andersen et al., 2015).The historic home range of CSTG once stretched from central British Columba, through half of Oregon and Washington, covering all but the highest peaks in Idaho, and large portions of central Utah, the northern parts of California and Nevada, and the western edges of Colorado, Wyoming, and Montana (Andersen et al., 2015; Buss & Dziedzic, 1955) (Figure 2). Buss & Dziedzic (1955) stated that by 1920, CSTG were only sited in areas of Washington where prairie and brush systems persisted. McDonald & Reese (1998) supported this finding in the latter half of the 20th century when they found that the decline in CSTG numbers in Washington was due in large part to the fragmentation and subsequent loss of grassland/shrub habitat. They also found that this same loss of habitat occurred throughout the entire Palouse region including those parts found in Idaho. The Palouse is a distinct geographic region of grasslands that cover parts of Washington, Idaho, and Oregon. Leupin (2003) reports similar findings in British Columbia, stating that Sharp-tailed grouse have been extirpated from grassland systems in the Pavillion ranges, east Kootenays (north and south of

Cranbrook), and from the Okanagan Valley. The core of the Canadian population is now isolated from populations in adjacent jurisdictions and confined almost entirely to the south-central interior of British Columbia.

Figure 2. Map showing historic and current range of CSTG. Current occupied range is located primarily in southeast Idaho and British Columbia indicated by dark grey. The areas of lighter grey indicate areas currently unoccupied by CSTG. (Andersen et al., 2015)

CSTG are dependent on a wide variety of vegetation and cover depending on the time of year (Andersen et al., 2015). Monitoring of Sharp-tailed grouse as they disperse throughout their range is difficult and often time consuming. Marks & Marks (1987) utilized GPS position radio collars to track birds but found the birds that had been fitted with GPS had a 100% predation rate. This may have been due to what is now outdated GPS collaring technology that was large and cumbersome to the movement of small birds.

2.2 Land Cover and Habitat Change

Globally, land cover and habitat change is responsible for the decline of most threatened and endangered species in peril. Krauss et al. (2010) stated that the intensification of agricultural land has led to a severe decline in semi-natural habitats across Europe. Plieninger supported Krauss' (2006) statements with a study in the south of Spain, finding that cultivated lands increased until 1975, when a shift was made to livestock production. Jetz et al. (2007) predicted that 950 to 1800 of the world's 8750 known species of land birds could be imperiled by climate change and land conversion by the year 2100. Jetz stated that climate change may influence range contractions at higher latitudes but the principle driver for effects on species will be land cover change. Skinner and Majorowicz (1999) correlated land cover change, from deforestation in the last century, to rises in surface temperatures in north-western North America. Wright et al. (2013) documented the western expansion of corn/soybean cropping and its replacement of grassland dominated ecosystems. Land use and land cover change are the most important factors causing biodiversity loss (Falcucci, Maiorano, & Boitani, 2007). Lambin et al. (2001) noted that land use change is happening at a global level, often driven by regions expanding into global markets. Lambin et al. (2001) further argued that markets drive land use conversions and that population growth, poverty, and infrastructure are too simple when considered individually to provide a complete picture of the drivers influencing land use change.

2.3 Multispectral and Hyperspectral Remote Sensing

Spectral imaging is a widely used tool for the detection and classification of vegetative communities. Vegetation yields a spectral response of reflected energy based on plant health, type, phenology, etc. Plant reflectance in the visible (400 – 700 nm), red-edge (680 – 730 nm), and infrared (700 – 1000 nm) wavelengths is typically used for vegetation classification. Numerous satellite platforms, including the National Aeronautics and Space Administration's (NASA) Landsat (series 1-8), the European Space Agency's Sentinel 2A and 2B, and Digital Globe's WorldView 2 and 3 space-borne sensors, provide multispectral imagery suitable for classifying vegetation and detecting land use and land cover change. Multispectral imagers typically have 3 -10 bands that consist of a broadband width (tens to hundreds of nanometers). In contrast, hyperspectral remote sensing, (i.e., narrowband) provides >10 spectral bands with narrower bandwidths. Liu et al. (2017) demonstrated hyperspectral's utility in the research of arctic vegetation, by discerning percent vegetative cover across a varying landscape.

Imagery from the Landsat TM, ETM+ and 8 and SPOT satellite instruments are able to separate land cover and vegetation types but insufficient at a fine scale for identifying individual plants on a species-by-species basis (Adam, Mutanga, & Rugege, 2010). According to Adam et al. (2010), this is due to three factors: (1) the difficulties faced in distinguishing fine, ecological divisions between certain vegetation species, (2) the broad nature of the spectral wavebands, with respect to the sharp ecological gradient of narrow vegetation units, in wetland ecosystems, and (3) The lack of high spectral and spatial resolution of optical multispectral imagery, which restricts the detection and mapping of vegetation types beneath a canopy of vegetation in densely vegetated areas.

Yu et al (2006) found that the accuracy of detailed vegetation classification with very high-resolution imagery was dependent on the sample size, sampling quality, classification framework, and ground vegetation distribution. Imagery classification relies on successful extraction of pure spectral signature for each species, which is often dictated by the spatial resolution of the observing sensor and the timing of observation (Xie, Sha, & Yu, 2008). It is possible to generate quantitative remote sensing data by means of a sUAS equipped with commercial off-the-shelf (COTS) multispectral and thermal imaging sensors (Berni, Zarco-Tejada, Suárez, González-Dugo, & Fereres, 2009).

Studies that apply the shortwave infrared (SWIR: 1400–2500 nm) wavelengths for estimating arctic biophysical variables are lacking (Liu et al., 2017). Further, spectral vegetation indices (VIs) designed for landscapes such as croplands, grasslands, and forests have seldom been tested for their utility in sparsely vegetated high arctic tundra with exposed soil/tills, large quantities of non-vascular plants (i.e. mosses, lichens), or large amounts of senescent vegetation (Liu et al., 2017). This is an important consideration when examining local Idaho landscapes. Vegetation in southeast Idaho is similar to arctic vegetation in that much of it consists of senesced, or dead, vegetation.

Vegetation indices remain the most efficient way of quantifying vegetation traits based upon hyperspectral images. According to Lucieer et al. (2014), VI's are the transformation of acquired reflectance spectra through mathematical combinations of purposely selected spectral bands that can maximize sensitivity towards biophysical or biochemical variables and simultaneously minimize effects of confounding environmental factors. There are a plethora of VI's that have been developed for classification (Table 1).

Table 1. Common Vegetation Indices

Vegetation Indices	Formula
NDVI	$\frac{(\rho_{\mathrm{NIR}} - \rho_{\mathrm{Red}})}{(\rho_{\mathrm{NIR}} + \rho_{\mathrm{Red}})}$
EVI	$G * \frac{(\rho_{\mathrm{NIR}} - \rho_{\mathrm{Red}})}{\rho_{\mathrm{NIR}} + \mathrm{C1} * \rho_{\mathrm{Red}} + \mathrm{C2} * \rho_{\mathrm{Blue}} + L}$
LAI	$(3.16 * EVI -).118)$
SAVI	$\frac{(1+L)(\rho_{\mathrm{NIR}} - \rho_{\mathrm{Red}})}{\rho_{\mathrm{NIR}} + \rho_{\mathrm{Red}} + L}$

The adoption of VI's, including the most widely used Naturalized Difference Vegetative Index (NDVI) and its refined form, Enhanced Vegetative Index (EVI), provide methods to map vegetation using optical remote sensing devices. The principle of applying NDVI in vegetation mapping is that vegetation is highly reflective in the near infrared bands and highly absorptive in the visible red bands. Xie et al (2008) demonstrated that the contrast between these channels can be used as an indicator of the status of the vegetation. Leaf area index (LAI) is also a key variable in canopy reflectance. Adam (2010) found that canopies with a high LAI reflect more than the canopies with medium or low LAI. Using LAI as one means of identification can be useful to researchers in areas with a large variation in leaf size between differing species.

2.4 Unmanned Aerial Systems and Wildlife

Wildlife managers and professionals are widely adopting the use of sUAS for research and monitoring purposes in natural systems. Rango et al. (2009) demonstrated the ability of sUAS to acquire high resolution (<6 cm) imagery with a subsequent vegetative classification accuracy as high as 92%. Sarda-Palomera et al. (2012) showed that sUAS are capable of performing surveys of ground-nesting birds, providing georeferenced nest locations without disturbing nesting individuals, something that cannot be accomplished by on the ground surveys. The issues, identified by Jones et al. (2006), of dealing with georeferencing and deployment have been addressed by the latest sUAS models. Small sUAS are now increasingly deployable and are decreasing in cost, with the added benefit of onboard georeferencing and a growing number of sensors that can be deployed on an airframe. In their review of sUAS for wildlife monitoring, Linchant et al. (2015) concluded that, though sUAS could benefit wildlife monitoring, the biggest barrier to adoption and deployment of sUAS would be legislation and regulation. Currently changes in regulations make it easier for researchers to integrate sUAS into their wildlife and habitat studies.

Chapter 3: The Effect of Land Cover Change on Measured Counts at Columbian Sharp-tailed Grouse Lek Sites

3.1 Introduction

Columbian Sharp-tailed Grouse (*Tympanuchus phasianellus columbianus,* CSTG) populations have been in decline since the mid to late 19th century and subsequently from land conversion since the turn of the 20th century (Buss & Dziedzic, 1955; Connelly et al., 2000; McDonald & Reese, 1998). Formerly, CSTG occupied a range from central British Columbia to California and Colorado (Marks & Marks, 1988). Historically, the habitats of CSTG were dominated by grasslands consisting of bunch grasses and sagebrush steppe (McDonald & Reese, 1998). Early 20th century settlement of CSTG home range resulted in increased mechanization of farming practices leading to an increase of cultivated acres (Buss & Dziedzic, 1955). An increase in cultivation leads to an increase of fragmentation of natural CSTG habitats. Habitat fragmentation has resulted in fewer CSTG populations consisting of multiple leks (McDonald & Reese, 1998). Excessive livestock grazing, overuse of herbicides, and burning of stubble fields has also had a negative impact on CSTG numbers (Giesen & Connelly, 1993). Idaho supports approximately 60-65% of the remaining CSTG in the U.S and is home to one of three populations that make up 95% of remaining breeding populations (Andersen et al., 2015).

CSTG rely on a diversity of vegetation communities for all life stages. Female nest site selection is dependent on available vegetation and corresponds to sites with a dense shrub cover for nesting success (Giesen & Connelly, 1993). For brooding, CSTG typically select areas with lower brush density that are dominated by species such as snowberry (*Symphoricarpos albus*) and sage (*Artemisia spp.*) (Klott & Lindzey, 1990). Male CSTG select lek sites located on knolls or ridgetops that are higher than surrounding areas. These sites have been characterized by a high abundance of native bunch grasses, and typically they include a much higher brushy component than sites selected by other sub-species of sharp-tailed grouse (Giesen & Connelly, 1993). There is limited evidence that dense cover on leks is detrimental to reproduction and survival of CSTG, but Klott & Lindzey (1990) reported less vegetative cover on lek sites than random sites.

Counts of males attending leks in the spring have been the primary means employed by states to monitor the status of grouse species (Mayer, 2008). Data on the population structure and dynamics are primarily obtained from these counts (Storch, 2007). In Idaho, the Idaho Department of Fish and Game and its cooperating partners have invested a substantial effort in conducting bird counts at lek sites; but they acknowledge that increasing the number of leks counted each year could strengthen current knowledge of population status (Andersen et al., 2015). While lek counts are the most widely used method for an indication of population trends, they can be problematic when not all leks are counted and there is a chance that not all birds attending a lek are recorded (Storch, 2007). Females disperse from a lek after breeding to lay their eggs and raise their young. The distance traveled varies but it is generally within 4 km of a lek site (Andersen et al., 2015). Many of the historic lek locations, and adjacent nesting and brooding areas lie within fields that are now under agricultural production (Andersen et al., 2015; Buss & Dziedzic, 1955; Giesen & Connelly, 1993; Storch, 2007).

This chapter explores the spatiotemporal relationships between yearly counts of CSTG at 69 lek sites and corresponding land cover change, focusing on the increase of agricultural land use between 2001 and 2016 in southeastern Idaho. The null hypothesis is that increases in agricultural land cover within 4 km of lek sites has no relationship to

CSTG bird counts at these leks. A preliminary analysis indicated the apparent increase in agricultural production was a driving factor in the decline of counts collected at lek sites. A deeper spatial analysis conducted through this research has indicated that the levels of change in agricultural production, at this temporal scale (2001-2016) and based on cover change assessment using the NLCD, cannot be determined as the influential factor in decreasing bird counts at lek sites.

3.2 Methods

3.2.1 Idaho Fish and Game Lek Count Dataset

The study area in southeastern Idaho includes Bannock, Oneida, and Power Counties (Figure 1). National Land Cover Dataset (NLCD) classifications from 2001 and 2016 were selected to compare to the Idaho Fish and Game (IDFG) supplied bird count data from leks recorded in their state database extending back to 1969. Lek surveys, which occur in late April, coincide with the time that male birds display on the lek. Each lek is visited at least three mornings within the counting period. Surveys begin 30 minutes before sunrise and continue until an hour and a half after sunrise. The lek bird count database from IDFG includes data from 318 leks within the three-county study area. To correspond to the NLCD land classification datasets and to allow for lag in the response of CSTG to changes in the landscape, I averaged bird count values taken+/- 2 years on either side of the years 2001 and 2016. If bird counts were completely missing in the dataset from 1999 to 2003 or from 2014 to 2018, I eliminated them from the survey. A minimum of one recorded count was needed during these two time periods to complete the analysis, even if the count was zero. The remaining number of leks for analysis was 69. The database consisted of information pertaining to state lek ID, longitude and latitude, and the values of the bird counts by year. I imported the lek dataset into a geodatabase within Esri's ArcGIS Pro. Projections for all data files within the GIS were set to the Idaho Transverse Mercator (IDTM) coordinate system, as this is the projection that IDFG utilizes for all GIS related data.

3.2.2 Land Cover Data

For this study, I used data from two national land cover programs. The Multi-Resolution Land Characteristics (MLRC) consortium's National Land Cover Datasets (NLCD) are 30 m resolution categorical data with a numeric value assigned to a pixel within the raster based on land cover type (e.g. Shrub/Steppe=52). The second dataset, the Rangeland Analysis Platform (RAP), was developed by the University of Montana, in collaboration with, the USDA's Natural Resources Conservation Service and the Department of Interior's Bureau of Land Management. This platform combines field plots from the land agencies' vegetation monitoring programs with historical satellite imagery to produce land cover products (30 m resolution) through machine learning. Both NLCD and RAP are products derived from Landsat imagery.

To prepare land cover change estimations within a regression analysis, I calculated the percentage of land cover type within a 4 km buffer of each lek site for 2001 and 2016. Female CSTG will travel an average of 4km distance from the time of lekking, to nesting and brooding, and then to wintering. I clipped The NLCD datasets for 2001 and 2016 to the lek buffers. Once clipped, I quantified the percentage of land cover type for cropland (agriculture), herbaceous cover, and shrub/steppe within each buffer.

3.2.3 Spatial Autocorrelation

Global Moran's I

Spatial Autocorrelation was tested using the Global Moran's I statistic. This statistic tests a dataset for clustering, randomness, or dispersion. This tool uses an attribute within the datasets, along with the geographic location to measure spatial autocorrelation. The five-year average bird count at lek sites around the target years of 2001 and 2016, as well as the percent change in agriculture production between the two time periods were tested to assess spatial autocorrelation. With all three runs, I selected the Euclidean distance method and a fixed distance band of 14 km to examine spatial autocorrelation within valley systems. Using Moran's, I, if the datasets are clustered or dispersed, the null hypothesis is rejected.

3.2.4 Regression Analysis

I entered the lek locations from the IDFG database into ArcGIS Pro and used a 4 km buffer to establish the area that is recognized as the nesting and breeding habitat for CTSG. The clipped NLCD raster for 2016 was subtracted from the clipped NLCD raster for 2001 to establish change classes for the time period. Performing a reclassification on the raster label values ensured that each subtraction would produce a unique value. The study area does not include all the classes that are available for the NLCD data, as only seven of the classes are present within the lek buffers. I built a table to record the change in class from 2001 to 2016. Simplifying the 12 classes yielded four classes: No Change/Non-habitat, Change to Agriculture, Change to Herbaceous, and Change to Shrub/Steppe. I calculated the percent change for each of the classes using the counts for each of the classes and the total cells within each lek raster. I then added values for percent change to the lek point feature class.

Ordinary Least Squares (OLS) regression evaluates the relationships between a dependent variable within a feature class and one or more explanatory variables. I used the amount of change in the bird survey counts at lek sites from 2001 to 2016 as the dependent variable with the percent change in agriculture, herbaceous, and shrub/steppe as explanatory variables, as well as the average slope and roughness (standard deviation of the DEM) for the 4 km buffer. The average percent shrub cover for 2016 was calculated from the RAP dataset and used as an explanatory variable as well. The DEM used for this analysis was the United States Geological Survey's National Elevation Dataset (NED), 1 arc-second (30 m resolution). OLS returned six assessments to validate the model, in this case the focus is on the correlations between the dependent variable and the explanatory variables.

3.2.5 EBK Regression Prediction

Empirical Bayesian Kriging (EBK) Regression Prediction is an interpolation method included with Esri's ArcGIS Pro. This tool uses EBK with explanatory variable rasters that represent data that is known (or thought) to affect the value of the data in question. The average percent slope, calculated from the NED DEM, along with the 2016 average percent shrub cover from the RAP, were utilized as explanatory rasters for this analysis. This tool also allows for moderately non-stationary data, thereby overcoming the considerations of normal kriging. The EBK Regression Prediction tool outputs a prediction layer as well as a geostatistical layer to generate rasters for standard error, quantile, or probability maps.

3.3 Results

3.3.1 Land Cover Change

Table 2 highlights the percent land cover change to agriculture, shrub steppe and herbaceous over the 2001 to 2016 time period. The table represents change across all 318 leks in Oneida, Bannock and Power counties and the 69 leks for which count data was available. In the table, agriculture was denoted by “Ag”, shrub/steppe by “SS”, herbaceous by “Herb”, and “Other” which identified all other classes that appeared in any of the buffered areas other than “developed”. “Other” classes included forest and open water. “Developed” were those areas that contained structures and hard surfaces. The percentage change to developed and other (0.00 and 0.01%) were not used for any other analysis. Figure 3 shows the locations of the 69 leks with an increase or decrease in the average count between 2001 and 2016. Within the black outlined buffered area is land cover converted to agricultural production between 2001 and 2016.

Table 2. Percentage of land cover change for all 318 leks in the three-county area and for 69 leks used for analysis

Class Change (2001-2016)	318 Leks	69 Leks
No Change	85.86	83.52
Percent Change to Agriculture (Ag)	**3.90**	**5.80**
Herb to Ag	0.61	0.68
SS to Ag	3.29	5.12
Other to Ag	0.00	0.00
Change to Shrub Steppe (SS)	**3.22**	**3.78**
Ag to SS	0.48	0.25
Other to SS	0.19	0.13
Herb to SS	2.55	3.40
Change to Herbaceous	**6.90**	**6.70**
Ag to herb	0.03	0.01
SS to herb	6.86	6.86
Other to herb	0.01	0.00
To developed	0.01	0.00
Other to Other	0.10	0.01

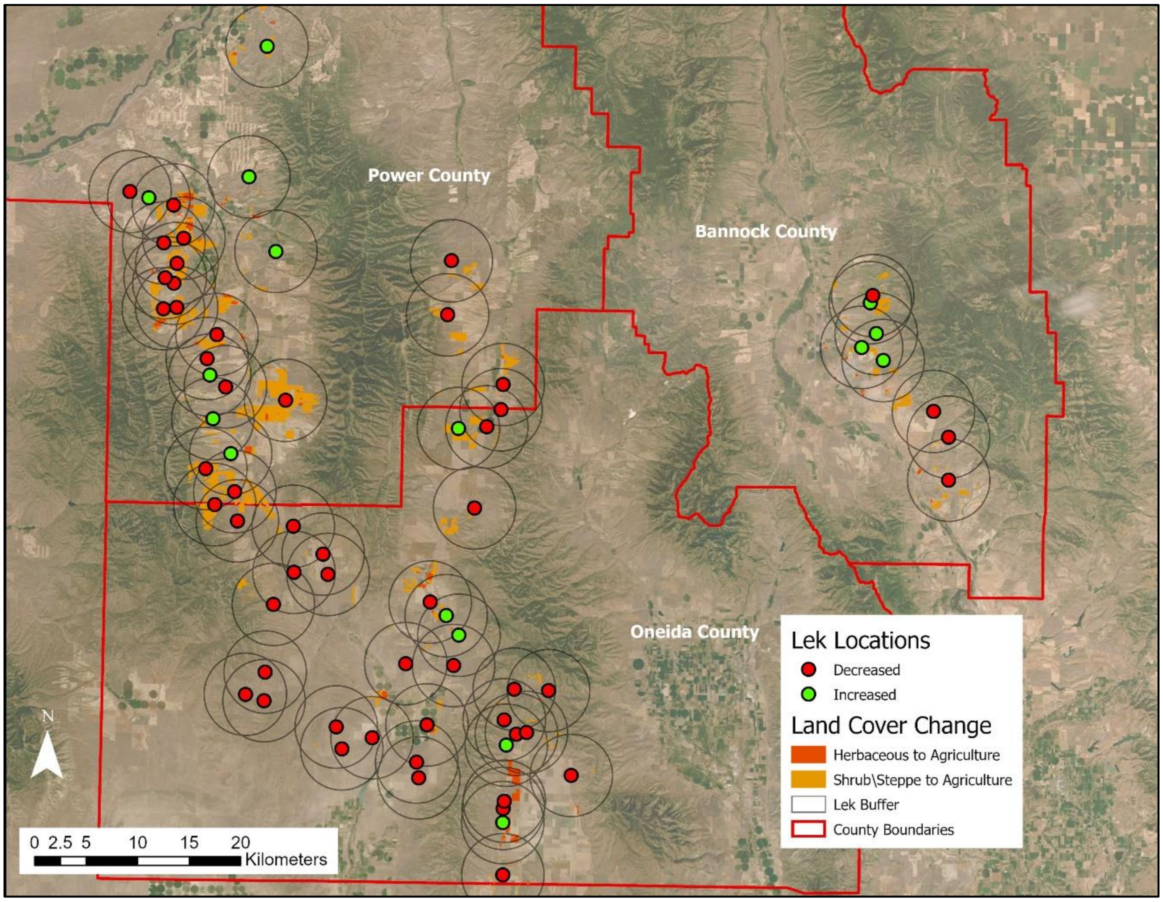

Figure 3. Lek locations for 69 investigated leks along with areas of land cover change to agriculture.

There were 16 leks out of the 69 that had an increase in the average count (2001-2016). One lek had an average value that remained unchanged between 2001 and 2016. Table 3 shows the values for the average of the counts for the two time periods (2014-2018 and 1999-2003), as well as the values for change in the count numbers for those leks, both increasing and decreasing.

Table 3. Average values for birds counted at lek sites for 2016 and 2001 and the amount of change for those counts.

	2016 (2014-2018)	2001 (1999-2003)	Leks with increased count	Leks with decreased count
n	69	69	16	52
Min	0 (average)	0 (average)	0.15 (change)	0.25 (change)
Max	33.5 (average)	30.6 (average)	26 (change)	29 (change)
Mean	6.35 (average)	10.79 (average)	7.55 (change)	8.2 (change)
σ	7.66	7.21	5.41	5.73
σ^2	58.95	50.96	29.32	32.85

3.3.2 Spatial Autocorrelation Results

Global Moran's I

The distribution for the lek's geographic location was random, the variable "Value of Change" represented the increase or decrease in averaged bird counts between 2001 and 2016 and returned a random distribution when tested (z = 1.08, p = 0 .27). The variable for percent change in agriculture was the only tested variable indicating a significant clustered spatial distribution (z = 9.33, p = 0.00, n = 69) (Table 4). Variables for both the average count of 2016 and the average count of 2001 indicated a clustered distribution, but the values were not statistically significant.

Table 4. Results of Spatial Autocorrelation (Global Moran's I)

Input Field	*z* score	*p* value	Moran’s Index
Value of Change	1.08	0.27	0.05
Percent Change in Agriculture	9.33	0.00	0.39
Average of 2016	-0.62	0.53	-0.04
Average of 2001	0.58	-0.54	-0.04

3.3.3 Regression

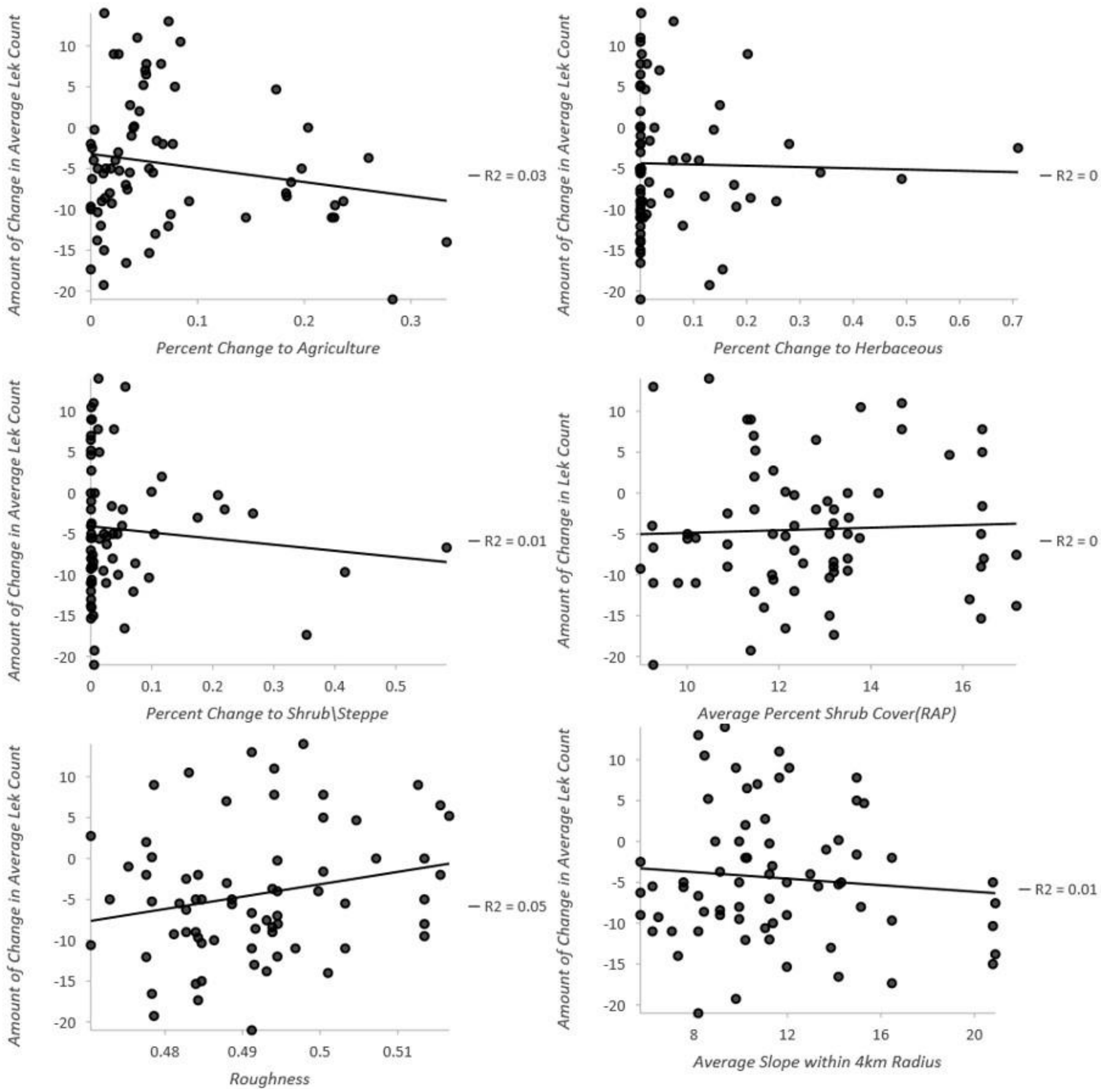

Figure 4. Correlation charts for average change in number of birds counted at lek sites vs. explanatory variables.

The regression analysis indicated that there was no strong relationship between the amount of change in the number of birds counted at lek sites and any of the tested explanatory variables (Figure 4). The percent change reported in change to agriculture, herbaceous, and shrub/steppe were all positive because they represent the percentage of the buffered areas that changed to their respective classes. The percent change in shrub/steppe from the RAP dataset is both positive and negative because it is the average percent change (increasing and/or decreasing) within the buffered areas.

3.3.4 EBK Regression Prediction

Figure 5 is a display of the results of EBK Regression Prediction. This analysis used the average percent slope located within each of the buffers as well as the average

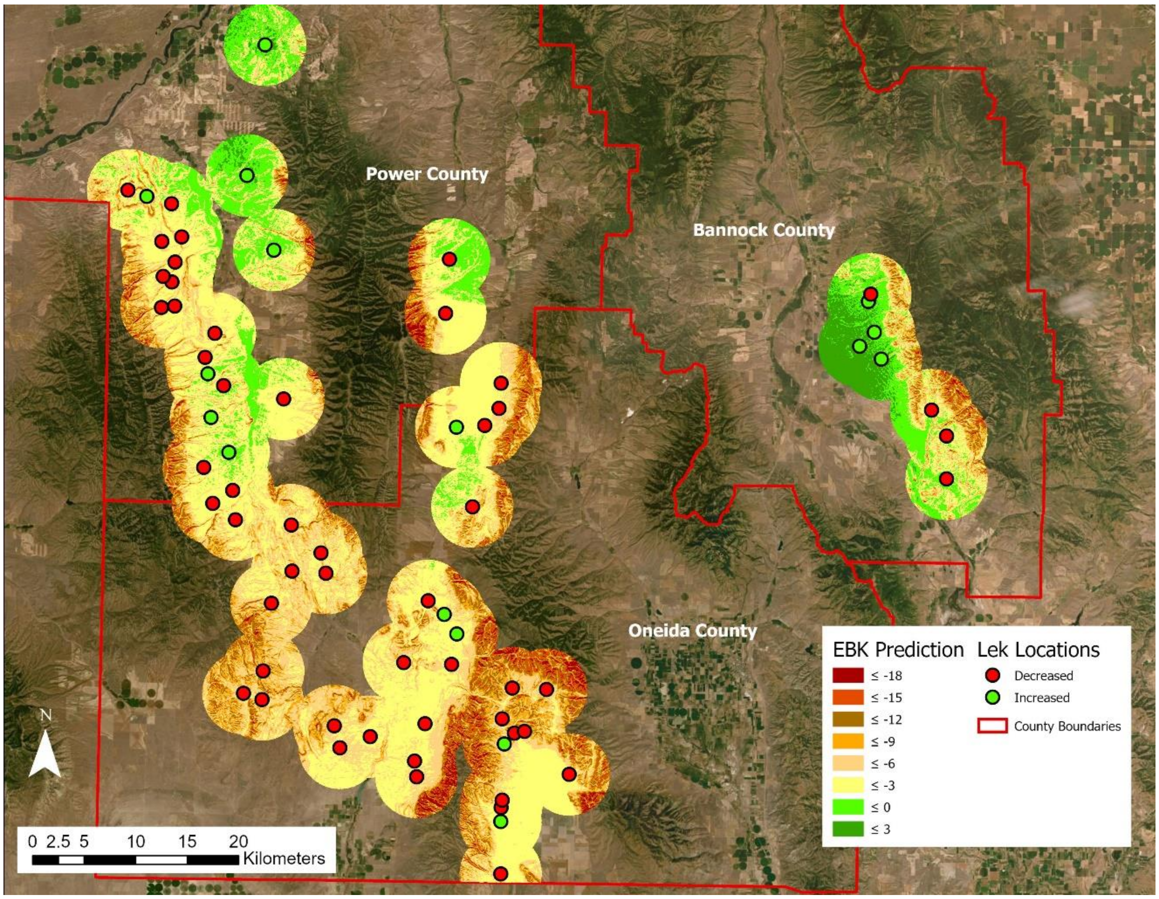

Figure 5. Results of Empirical Bayesian Kriging Regression Prediction.

percent shrub cover from the RAP dataset. The green areas of the map that indicated where the model predicted a possible increase to lek count numbers. Areas in yellow and red were locations where number of birds counted at lek sites may be decreasing at varying rates. Lek locations indicated where the 69 leks used for analysis were located and whether their average count from 2001 to 2016 was increasing or decreasing.

3.4 Discussion

This chapter provides an investigation into the relationship between bird counts at lek sites and land cover change in southeastern Idaho. For this study, a visual comparison between the 30 m resolution NLCD datasets to corresponding years of 1m resolution National Agriculture Imagery Program (NAIP) data revealed poor accuracy in land cover classification. This level of discrepancy may be high enough to raise concern regarding assumptions about populations based upon NLCD data. For example, Figure 6 highlights one of many examples discovered in the 2001 and 2016 NLCD datasets where large areas misclassified agriculture and shrub/steppe.

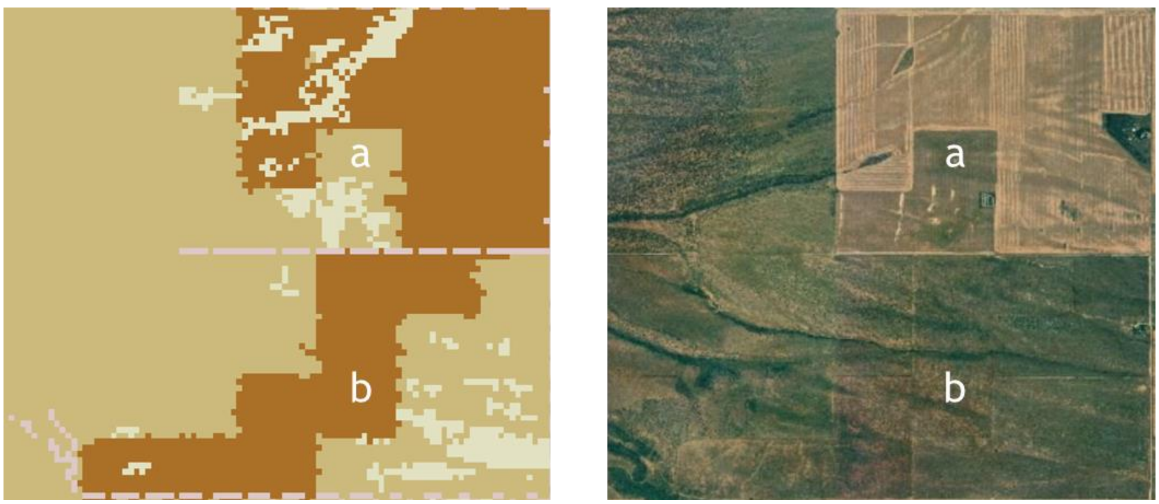

Figure 6. NLCD Classification (2011) vs. Natural Color NAIP (2011) image of same area. Location "a" is a crop field that is classified as shrub/steppe and location "b" is shrub/steppe classified as cropland.

Landsat imagery, upon which the NCLD is based, has the one of the longest temporal records of space borne sensors (1972 to present). The launch of Landsat 5 (1984), which carried with it a Multi Spectral Scanner (MSS) as well as a Thematic Mapper, nearly coincided with the passing of the 1985 Farm Bill and the introduction of conservation reserve programs in these areas. Because initial investigations have pointed heavily toward agricultural fields having the largest influence on the decline of bird counts at lek sites, it is recommended that further work focus on accurately classifying land cover over this time period to better discern between areas that are in agricultural production and those that are not. Improved accuracy in land cover assessments will increase confidence in reported land cover change and response of bird populations.

The NLCD only goes back until 2001. Recently the MRLC has supplemented the original time step of every five years by completing classifications every two or three years. Even so, the time span from 2001 to 2016 seems too small to measure the amount of land cover change as the amount of land cover change (2001-2016) from any class to agriculture was relatively low (3.9%). In fact, it was nearly as low as the amount of ground converted to shrub/steppe (3.2%) over the same time period. Concurrently, the areas that changed to herbaceous cover were nearly twice as high (6.9%). Several factors may account for this finding.

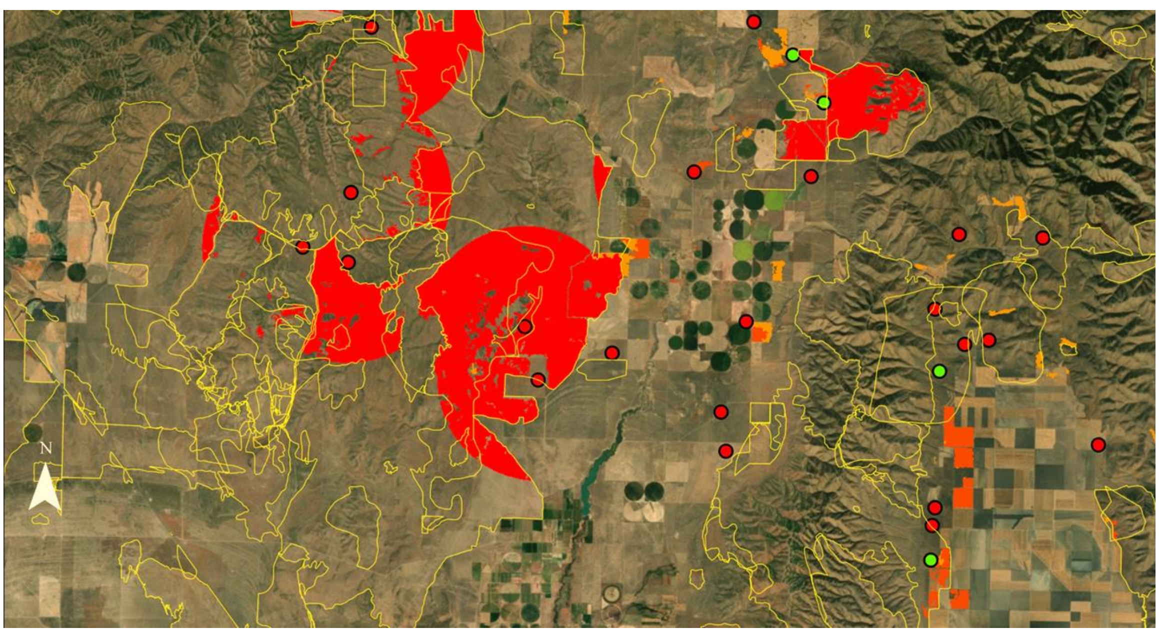

Figure 7. Land conversion to herbaceous/grassy class is shown here in red. Most of the conversion in the southern part of Power county coincided with historical fire boundaries outlined in yellow

One is the misclassification of agriculture and shrub/steppe, already mentioned, and the other is the abundance of wildfire that has occurred in some of the historical shrub/steppe ecosystems. Most of the conversion from shrub/steppe to herbaceous within the 4 km buffers surrounding the leks correspond to historic fire boundaries (Figure 7). CSTG population decline has spanned almost 1.5 centuries, but for this study, I only used data and imagery for the last two decades.

Although the results from the OLS regression analysis returned low correlation values, I used the EBK Regression Prediction tool to examine change in bird counts at lek sites with the change in the percent of shrub cover as an explanatory variable. This process predicted the areas where lek count numbers were changing. A visual comparison of the areas where landcover change occurred suggested that there is a decrease in birds counted at those leks that are closer to areas that had an increase agriculture and to areas that had an increase in grassy cover. Those areas that have increasing average number of birds counted at lek sites correspond to areas that the EBK Regression Prediction was suggesting should have increasing lek count numbers and vice versa.

The bird counts at lek sites database is problematic in that many leks have large gaps between years counted. The low number of lek locations (n = 69) used in this study is due to the lack of count records and may have skewed the regression analysis. I used Ordinary Least Squares regression and Empirical Bayesian Kriging Regression Prediction to test the correlation of the number of birds counted at lek sites with landcover change. The low number of lek sites that had data for the time period being investigated, limited the ability of OLS to correlate variables. I believe with a richer lek dataset and a more accurate imagery classification both OLS and EBK would be able to indicate the variables responsible for CSTG numbers. This will inform future research regarding the use of NCLD classified imagery to explain lek locations and numbers. Research in this area will further the knowledge of past management to inform new approaches to site counts and land cover datasets to better manage CSTG populations.

Chapter 4: Utilization of Small Unmanned Aerial Systems to Map Columbian Sharp-tailed Grouse Nesting and Brood Rearing Habitats in Fields Managed for Conservation

4.1 Introduction

Columbian Sharp-tailed grouse hens select areas for nesting and brood-rearing that are in close proximity to lek sites (Giesen & Connelly, 1993). For this reason, researchers often center habitat studies on the leks. A large number of leks occur in lands that are enrolled in conservation programs. The United States Department of Agriculture's (USDA) Conservation Reserve Program (CRP) serves to reduce soil erosion, improve water quality, and create or enhance wildlife habitat by growing food and cover. There are several practices within CRP to promote higher quality natural habitats for wildlife species. An example is sowing fields with native cool season grasses along with forbs and legumes that grow primarily in spring, early summer, and fall. These grasses are generally stiff, upright and grow primarily in bunches, which provide excellent nesting and winter cover. Natural communities are also associated with native legumes, forbs, and shrubs. Legumes and forbs provide sources of food for pollinators, viable seeds, and insect sources for young birds. CSTG hens prefer these fields for their resources during nesting and brooding periods, as well as for winter habitat.

Fields within the CRP program play an important role in the management of CSTG. Because southeast Idaho holds one of the last remaining breeding populations of CSTG, participation by landowners in land rehabilitation and restoration is key to the survival of CSTG. In order to make the best decisions for the longevity of CSTG, land managers need to have information about vegetative composition in areas utilized by the species. This study utilizes a small unmanned aerial platform equipped with a hyperspectral imaging system to map and quantify vegetation composition on CRP fields located within a 4 km radius of leks. The goal of this research is to validate the utility of mapping and classifying vegetation at high spatial resolution, and to generate best practices for the capture of high-resolution imagery.

Small Unmanned Aerial Systems (sUAS) have recently emerged as a new technology for use in wildlife and conservation management. sUAS platforms have the ability to carry sensors that include digital cameras, spectral imagers, LiDAR systems, and even radar (Costa et al., 2012; Jensen, Austin M.; Baumann, Marc; Chen, 2008; Zaugg, Edwards, & Margulis, 2010; Zhang & Kovacs, 2012). With the multitude of sensors available and a continual size and weight reduction of sensors and payloads, sUAS are replacing conventional observations and manned aerial surveys. For example, to obtain population size of Black Gull colonies, with similar accuracy to ground counts and without disturbing the colonies, researchers deployed sUAS to obtain georeferenced images from which they could identify and count individual birds in the colony (Sardà-Palomera et al., 2012). Surveys from sUAS can bridge the gap between ground-based rangeland measurements and remotely sensed imagery from piloted aerial or satellite platforms, both in terms of image scale and image acquisition costs. sUAS have several advantages over piloted aircraft. sUAS can be deployed quickly and repeatedly (Laliberte, Winters, & Rango, 2011). Van Blyenburg (2013) identified 406 imaging and ranging instruments developed specifically for sUAS including active and passive systems, microwave systems, and optical sensors from visible band to Near Infrared (NIR) up to Thermal Infrared (TIR). sUAS presents an accurate and cost effective method for mapping critical ecosystems (Boon, Greenfield, & Tesfamichael, 2016). Due to their low cost and operating expenses, plus their suitability for remote sensing, predictions are for small sUAS to have broad use across the resource management sector Many of the image processing steps have their origins in traditional aerial image processing and analysis. Photogrammetric processes have been implemented with sUAS collected data to produce fine scale, high precision mapping products (Colomina & Molina, 2014). Inexpensive sUAS coupled with Structure from Motion (SfM) can also produce ultra-fine scale classification maps, which have the potential to drastically change the scientific understanding of ecological systems (Cunliffe, Brazier, & Anderson, 2016). Boon (2016) showed the utility of high resolution sUAS imagery to map critical wetlands areas that would be difficult to access on foot. High resolution sUAS imagery has also been used to assess biodiversity in forested areas (Getzin, Wiegand, & Schöning, 2012).

Although high resolution natural color imagery has lent itself to the development of many habitat assessment products, Hyperspectral imagers (HSI) are considered the sensors of choice for mapping and monitoring vegetation (Adam et al., 2010). Compared with multispectral systems, which only have a dozen spectral bands, hyperspectral imagers may have hundreds of spectral bands (Xie et al., 2008). The greater spectral resolution of hyperspectral sensors allows in-depth examination and discrimination of vegetation types that would be lost with other multispectral platforms (Adam et al., 2010). Ouerghemmi et al.(2018) demonstrated that the use of a hyperspectral imager resulted in a significantly better ability to differentiate between individual tree species.

Hyperspectral imagers also have the ability to be tuned to examine specific wavelengths of the electromagnetic spectrum (Mozgeris et al., 2018). This “tunability” is a huge factor when dealing with vegetation that is highly responsive in the Red-Edge (680-

730 nm) to Near Infrared wavelengths (780-2500 nm). Only in the last decade has hyperspectral imaging systems become small enough and light enough for deployment on a sUAS (Nackaerts, Everaerts, Michiels, Holmlund, & Saari, 2010).

4.2 Methods

4.2.1 Study area

The study area is near Downey, Idaho. Six fields, roughly 65 hectares each (390 ha total) (Figure 8) were selected for their proximity to known lek locations and because they were in Idaho's Conservation Resource Program (CRP), whose goal is to promote vegetation rehabilitation to a more natural state. Rehabilitation management of each field ranges from 2 to over 20 years (Table 5). The site is in a shrub steppe area with vegetation composition ranging from sagebrush (*Artemisia spp*.) and rabbit brush, (*Chrysothamnus spp*.) to large forbs such as sainfoin (*Onobrychis viciifolia* Scop.) and alfalfa (*Medicago sativa*) to small forbs and grasses. The ground surface is typically gently rolling hills with some steeper drainages. CRP has many practices that are available to property owners for land enrollment. The fields flown are managed under general CRP, pollinator habitat improvement guidelines, and the State Acres For wildlife Enhancement (SAFE) practices. All CRP practices originate in soil erosion control, but specialized practices like pollinator habitats and SAFE have the added benefit of establishing or enhancing wildlife communities.

Table 5. Fields flown by sUAS.

Field	Date Flown	Area (hectares)	First Year in CRP	CRP Program Type
H	July 3, 5	59	1997	General
DM	July 17, 18	68	2015	Pollinator
DS	July 6, 9	60	2016	Pollinator
DN	June 11, 12	64	2010	Pollinator
DB	June 25, 27	65	2010	Pollinator
T	July 10, 11	65	1997	SAFE

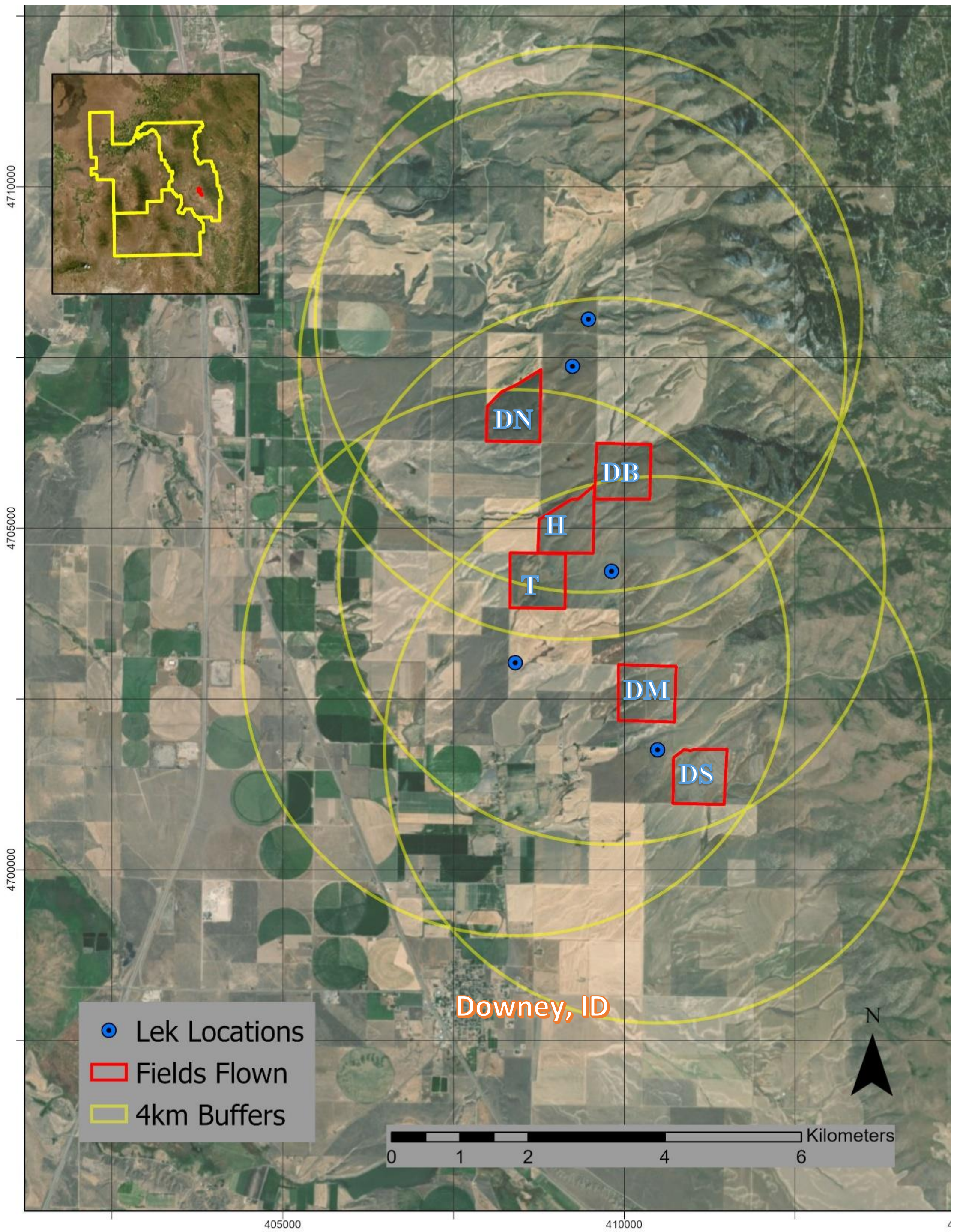

Figure 8. Study area near Downey, Idaho. Fields flown are outlined in red. Lek sites are indicated by blue dots with 4km radius lek buffers being shown by yellow circles. Downey is seen in the center near the southern edge of the map.

Figure 9. DJI Matrice 600 Pro equipped with hyperspectral imager (a) and digital camera (b).

4.2.2 Imaging system

This project followed similar workflows established by Mozgeris et al. (2018) and Ouerghemmi (2018). The imaging system utilized in this study consisted of two sensors and a UAV platform (Figure 10). The UAV platform was the Matrice 600 Pro hexacopter (Figure 9) produced by DJI Technology Co., Ltd., (DJI, Shenzhen, China). An automatic piloting system, with a piloted backup, controlled the hexacopter. A Ricoh GR II 16-

megapixel digital camera captured natural color images. The Ricoh GRII has a 23.7 x 15.7 mm CMOS sensor and a 28 mm (35mm equivalent) focal length. Image capture was in RAW format with autofocusing and auto white balance control. The digital camera triggered every 2 seconds to capture an image. Image size for the digital camera was 4928×3264 pixels producing a field of view (FOV) of 97.1 m x 63.9 m at 75 m above ground level (AGL).

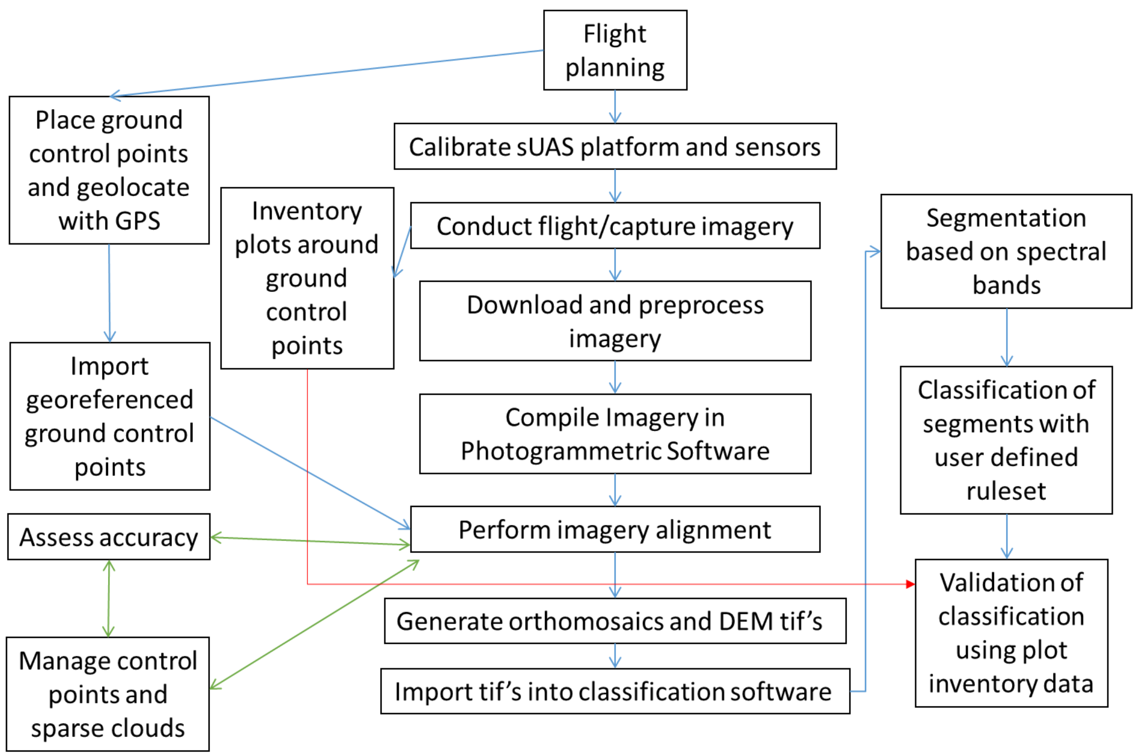

Figure 10. Workflow for HSI equipped sUAS

The second sensor was the Rikola Hyperspectral Imager (HSI). The HSI is a frame type imager that provides a real spectral response in each pixel over a range from 500-900 nm. I programmed the HSI to cover spectral bands from 599 to 870 with an average distance of 18 nm between bands. The HSI triggered every three seconds; the resulting image size was 1010x1010 pixels, producing a FOV of 45.8 x 45.8m at 75m AGL. The

HSI has its own GPS receiver that plugs into the sensor body, allowing for georeferenced images. The digital camera does not have an internal GPS, so images are georeferenced after the flight using the UgCS built-in function to match the time stamp from the digital camera to the recorded telemetry from the UAV's GPS location.

Both sensors were hard mounted in nadir configuration, to the bottom of the UAV platform using an in-house fabricated mount (Figure 9).

4.2.3 Ground Control Points and Scale Bars

Prior to flying, ground control points were positioned in each field using paper plates as targets (Figure 11). These points were set near to the corners of the fields and randomly distributed throughout the interior of fields. The corners of the fields were georeferenced to reduce error and aid in the photogrammetric and structure from motion processing. Each field had eight to ten ground control points. After a flight, each plate was georeferenced using a Trimble GeoXH 6000 series, handheld GNSS device. Inventory and layout of every 4 m^2 and 10 m^2 plot with each plot center marked with a paper plate. Placing 1m scale bars on the ground during flights aided in imagery processing.

Figure 11. Ground control plate with 1m PVC frame used for plot inventory.

4.2.4 Image Acquisition

Image acquisition took place over several days in June and July of 2018 (Table 5). I divided each field into seven to ten flights. Because the HSI image FOV at 75 m AGL is smaller than the digital camera (45.8 x 45.8 m vs 97.1 x 63.9 m), I planned overlap and side-lap images based upon the smaller sensor size. Selecting an overlap of 75% and a side-lap of 35% percent maximized the coverage of the HSI images. The overlap and side-lap on the digital camera exceeded 95% each. The resulting resolution for the acquired original images was 0.05 m for the HSI and 0.02 m for the digital camera. The HSI captured 16 spectral bands, from 599 to 900 nm with an average distance between bands of approximately 18 nm (Table 6).

Table 6. Hyperspectral Camera Band Configuration

Band	Central Wavelength (nm)	FWHM (nm)
1	599	11.7
2	617	10.5
3	636	11.4
4	653	10.1
5	671	20.1
6	690	18.2
7	707	19.2
8	726	17.6
9	743	16.7
10	761	15.2
11	780	14.9
12	798	15
13	815	14.4
14	833	14.4
15	851	13.4
16	870	13.5

Prior to each flight, a series of spectral references had to be captured both for light and dark references. These references serve to normalize the radiometric signature as lighting conditions change in between flights and throughout the day. I captured light references by aiming the HSI at a Spectralon calibration target with a known 99% reflectance value. I captured dark references by covering the lens of the HSI so no light could infiltrate the image. Flight planning was done in Universal Ground Control Software (UgCS), developed by SPH Engineering, Latvia. I planned flights at an above ground altitude of 75 m. Each field was roughly 65 ha. Flights were approximately fifteen minutes each, consisting of four passes at 45.8 m in width to cover the length of the field (800m) using a simple grid pattern. Each flight would cover ten to eleven hectares. Most fields took two to three days to get complete coverage. Flights occurred from 10:00 am to 4:00

pm to minimize the amount of shadows in the imagery. Flight speeds were set to 4 m/s. I flew on days with full sun and wind less than 4 meters per second. There were some instances when cumulous clouds would cover parts of the field during a flight, resulting in shaded areas in the imagery.

4.2.5 Image Processing

I shot the images from the digital camera in RAW, which allows for correction of white balance and exposure errors in the imagery. I corrected the RAW images for tone and white balance in Adobe Lightroom and exported as tagged image file format (TIFF). Because the digital camera's FOV is larger and I captured images at a shorter interval, there were almost twice as many images as were captured with the HSI. I removed blurry and poorly exposed images before processing without creating voids in the coverage. I used Agisoft Metashape for photogrammetric processing. Georeferenced ground control points and scale bars provided a means to more accurately ortho-rectify photos and to generate ortho-mosaics and digital elevation models (DEM) for each field. Images on the edges of the flight paths did not have adequate overlapping coverage to produce low error outputs. For that reason, I planned flight areas large enough to cover the entire field with over-run on the sides and ends so I could trim the resulting ortho-mosaic and DEM in ArcGIS Pro to remove areas that were distorted.

The HSI camera produces k-type raw hypercubes with associated metadata, as well as the task file containing information needed to compile the hypercube from raw data. The k-type hypercube is a data cube consisting of images form all 16 bands captured when the camera is triggered one time. Hypercubes were pre-processed using the included software tools from the camera manufacturer. These tools convert the image digital number values into radiance values. I then converted each band into 16-bit TIFF files, resulting in 16 images per hypercube. I combined the 16 hyperspectral bands into a 16 band GEOTIFF using the Composite Bands tool in ArcGIS Pro 2.3.

4.3.5 Image Classification

I imported the composite TIFFs, DEMs, and ortho-mosaics into Trimble's eCognition Developer software for classification as image layers. eCognition allows the user to perform an object-oriented classification by defining a set of rules based upon observations made for each of the individual layers within the project. The first step within the process was multi-resolution segmentation. The segmentation looks at all the layers within the project and groups individual pixels that have similar attributes together into polygons with size and shape adjusted by the user.

After the segmentation process, each segmented area had a mean value associated with it for each of the image layers within the project. Other layer attributes were user-defined within the software, including proximity to other classes, band indices, shape, size, etc. I extracted and plotted spectral curves for individual plants (Figure 12). Each curve represented the spectral signal for one of the classes. I calculated class values for each of the images captured wavelengths by taking an average for each wavelength captured from 50 polygon segments that had been assigned to each class.

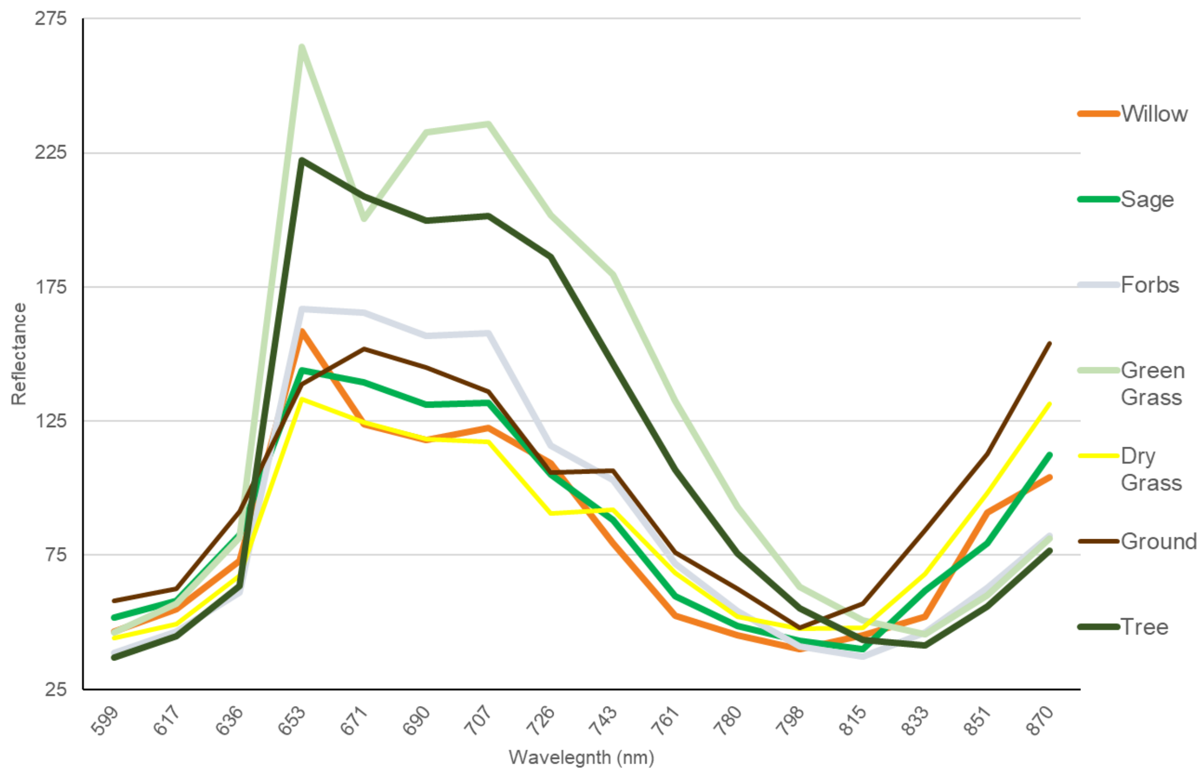

Figure 12. Spectral signature of defined classes.

Classes were defined based upon one or more attributes for physically and spectrally similar polygons (Table 7). I used the rule set to classify all the polygons within the project. This rule set classified each pixel into one of eight classes: tree, willow, sage, bare soil, green grass, forb, dry grass, and brush. Once the classification was completed, polygon shapefiles that contained the classification attributes were exported to be viewed in ArcGIS Pro.

Table 7. Ruleset used to define classes in eCognition software.

Rule	Outcome
First segmentation	Creates large segment polygons of Rough classes
NDVI, Band 690, and Band 870 and Relative border	Defines rough class as Forb, Willow, or DryGrass
Second Segmentation	Creates small segment polygons within each Rough class
DEM Standard Deviation (SD) > 0.2 and Height model > 1.5 m	Define Tree Final class
Brightness < 35	Define Shadow Final class
Brightness > 175 and DEM SD < 0.02	Define Bare Final class
DEM SD >= 0.02 and < 0.04	Shrub Secondary class
DEM SD >= 0.04	Tall Shrub Secondary class
Tall Shrub Band 671 > 115 and < 160, and Band 690 >110	To Sage Final class
Relative Border to Sage > 0	To Sage Final class
Forb and DryGrass Band 653 > 180, 671 > 180 and 690 > 180	Define GreenGrass Final class
Relative Borders > 0.3	To respective final classes
Merge Regions	Merges like classes into polygons for export
Export	Exports segments as shapefile for ArcGIS Pro

4.3.6 Accuracy Assessments

The resulting classification polygons were brought into ArcGIS Pro and the georeferenced plot sites were imported, buffered, and had Feature Envelope to Polygon run on them to generate plots that measured 100 m^2 and 4 m^2, corresponding with the inventories taken at the time the plots were geolocated. A fishnet was generated that covered the entire field, with squares measuring 10 cm x 10 cm. The Fishnet was then clipped to these plots and a spatial join was completed to associate the classification information with the individual 100 cm^2 squares of the fishnet. The plot inventories were overlaid with a similar fishnet grid that matched the size of the classification fishnet. When plots were inventoried, the locations were such that there were no plots that contained the classes tree and willow. Pixel class values from fifty points were selected from the classification grid and compared to values of corresponding locations within the inventoried grid to generate a confusion matrix from each of the six remaining. I chose a total of 300 pixels for each of the fields. The tree class and the willow class did not occur within the inventoried plots, but because of their unique spectral signature, their physical characteristics, and the ease of which these types of vegetation are visually identified, I was able to include these two classes in the classification. Confusion matrices were used to assess accuracy, or the percentage of pixels that were correctly predicted by the model. Accuracies were determined by identifying the number of true positives, true negatives, false positives, and false negatives (Table 8).

To calculate accuracies, the number of pixels that were correctly classified (true positive + true negative) were divided by the sum of true positive, true negative, false positive and false negative predictions. I computed accuracies for all combined areas: each field, each class in all combined areas, and each class in each field.

Table 8. Definitions for matrix outcomes.

Matrix Outcome	Definition
True Positive	Pixels correctly classified as belonging to the class
True Negative	Pixels correctly classified as **not** belonging to the class
False Positive	Pixels **incorrectly** classified as belonging to the class
False negative	Pixels **incorrectly** classified as **not** belonging to the class

4.4 Results

Each of the six fields in the study area produced several remote sensing products that included a three-dimensional elevation model and a natural color image from the RGB camera in addition to a sixteen-band composite, hyperspectral orthoimage. Agisoft Metashape minimized georeferencing errors with typical accuracies being less than 5 cm for the models generated from the digital camera. The spectral imagery had a wider range of accuracies, but still averaged near the 5 cm mark. Some of the composite band spectral images saw more distortion in areas where ground control was limited.

Classification accuracies ranged for each of the fields (Table 9). The fields produced an average accuracy of 77.18%. Field DB had the highest overall accuracy at 86.16%. The overall accuracies considered all the classes in the model. When each class was considered on an individual basis, classification accuracies were greater than 74.5% on average for each class, with bare soil being the highest at 82.6%.

The resulting classification images (Figure 13-Figure 16) illustrate the mapped vegetation across the four fields analyzed. Table 10 through Table 13 shows the area of each of the classes and the percentage of the field that the class occupies.

Table 9. Classification accuracies calculated from confusion matrices.

Field	Class					
	Forb	Sage	DryGrass	GreenGrass	BareSoil	Brush
DB	86.5%	86.5%	85.8%	84.0%	90.9%	83.3%
DM	77.2%	75.4%	76.8%	79.6%	79.6%	76.1%
H	81.5%	80.7%	81.1%	81.1%	89.3%	80.7%
T	71.2%	70.1%	70.8%	77.3%	74.3%	75.1%
Mean	74.5%	75.4%	75.4%	78.9%	82.6%	76.3%

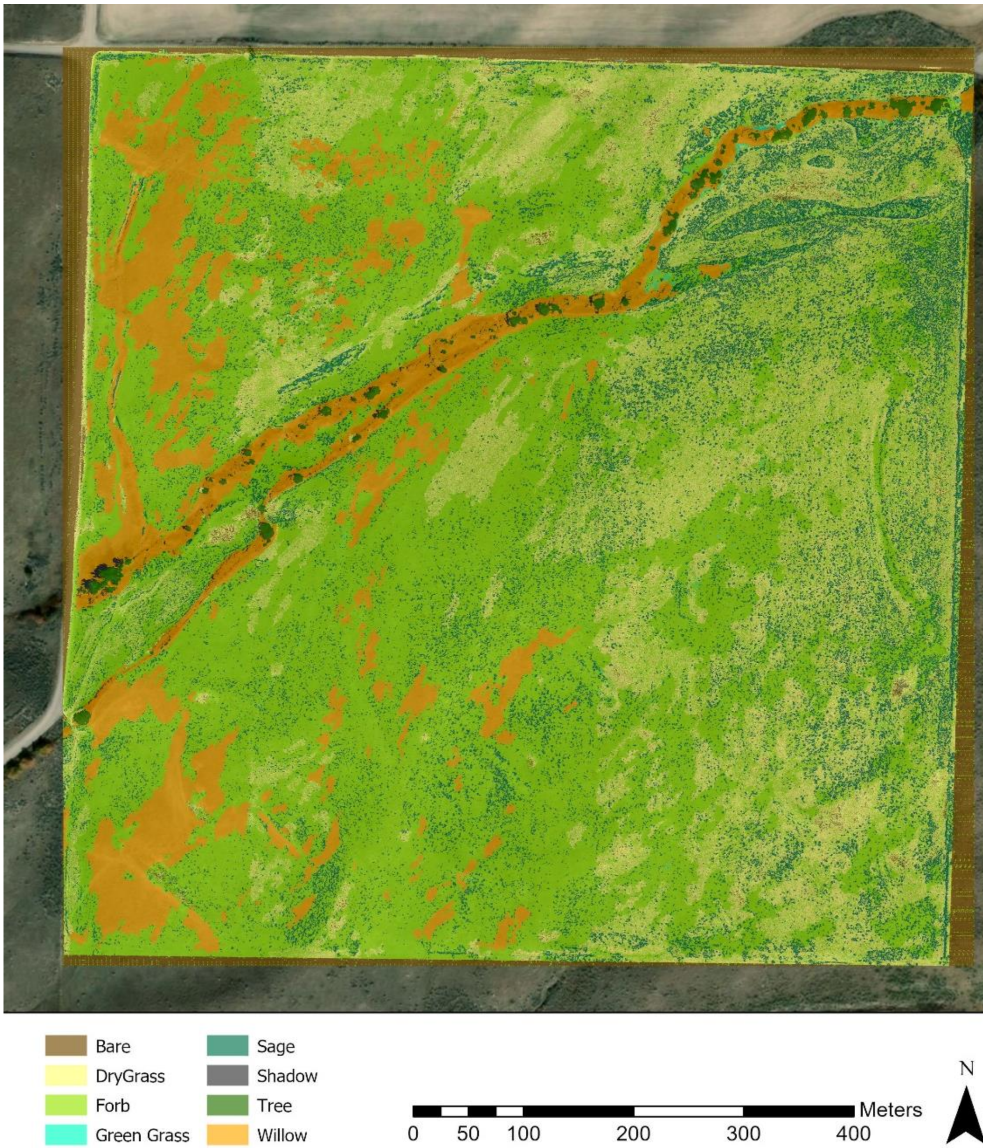

Figure 13. Classification result for field DB

Table 10. Field DB classification results area and percentage of field.

Class	Area (ha)	Percent of Field
Bare	3.95	5.72%
DryGrass	11.21	16.24%
Forb	36.73	53.22%
Green Grass	0.14	0.20%
Sage	8.63	12.51%
Shadow	0.14	0.20%
Tree	0.37	0.53%
Willow	7.86	11.38%

Figure 14. Field DM classification results.

Table 11. Field DM classification results area and percentage of field.

Class	Area (ha)	Percentage of Field
Bare	3.80	5.52%
DryGrass	11.30	16.40%
Forb	44.74	64.92%
Green Grass	0.01	0.02%
Sage	7.81	11.33%
Shadow	0.03	0.04%
Tree	0.40	0.59%
Willow	0.82	1.19%

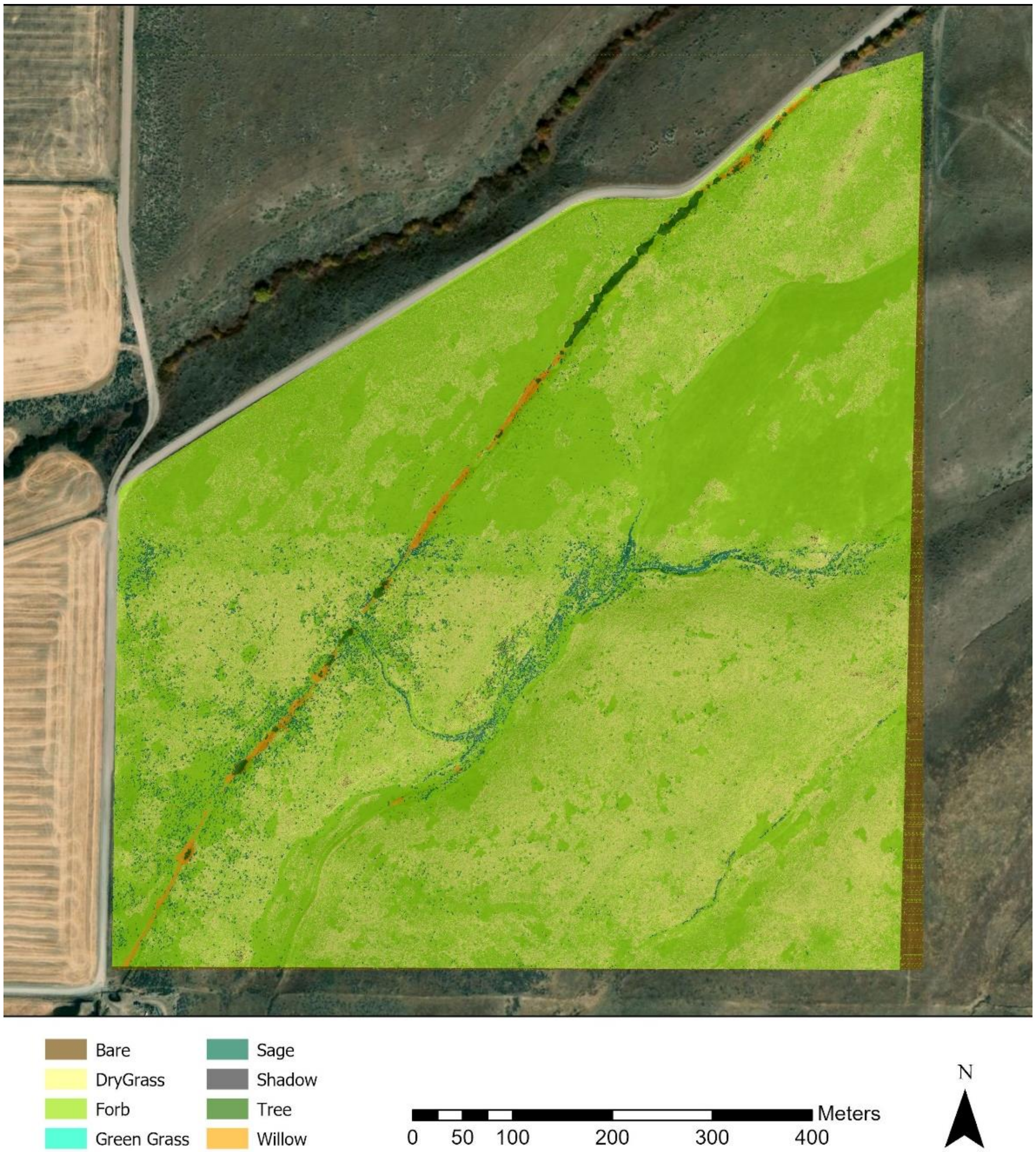

Figure 15. Field H classification results

Table 12. Field H classification results area and percentage of field.

Class	Area (ha)	Percentage of Field
Bare	1.41	2.44%
DryGrass	16.55047	28.63%
Forb	37.4268	64.74%
Green Grass	0.004725	0.01%
Sage	1.83532	3.17%
Shadow	0.010953	0.02%
Tree	0.244191	0.42%
Willow	0.328156	0.57%

Figure 16. Field T classification results

Table 13. Field T classification results area and field percentage

Class	Area (ha)	Percentage of Field
Bare	2.50	3.74%
DryGrass	23.09	34.50%
Forb	26.99	40.32%
Green Grass	0.47	0.70%
Sage	13.46	20.10%
Shadow	0.00	0.00%
Tree	0.00	0.00%
Willow	0.43	0.64%

4.5 Discussion

The map layer products created during the photogrammetric and structure from motion processes of this project have a resolution and repeatability that cannot currently be gained from satellite borne sensors. The ultra-fine scale resolution (xx cm) is a huge benefit for mapping and identification of plant communities. Individual plants as small as several centimeters can be identified from the imagery. The classification software and model can handle imagery at this fine scale. One limitation was problems in the co-registering of spectral bands. In areas where the bands were nearly perfectly aligned, the classification model performed relatively well, but in areas where the bands were shifted in the geolocation of coincident pixels the classification model would fail. This is because the classification model is based upon looking at all layers at the same time and analyzing the layer characteristics of several layers for each of the classes developed.

The model performed better on some classes than it did on others. Classes such as bare soil, which has a spectral signature that is distinct from any vegetation signal, had a higher accuracy in prediction than any of the other classes. Vegetation signals were hard to separate at some wavelengths because of the similarity between the spectral signal of some plant types. Segments that contained sage appeared to be spectrally different than segments that contained other types of brush. Segments that contained some sort of vegetation that was green were more difficult to distinguish between species.

Ideally, one ruleset would classify all images. To test this, I applied the same classification rule set for all the fields. There were only slight modifications made to the algorithm in eCognition to get the model to run properly and classify the images. These refinements did not alter the basic ruleset. Field DB, which was flown in late June, was used to develop the initial ruleset, because I thought that it would provide a better representation of early summer vegetation's spectral signal. The accuracies of the fields that flown closer to the date of that field were higher than the fields flown more than a week before or after that field was flown. This points to the changing of the spectral signature within vegetation as plants were greener in weeks prior to the model and drier in the weeks after. The very first field that was flown (Field DN), was flown in early June and had an observable difference in the amount of green growing vegetation than the subsequent flights. This field was the one that did not have plots inventoried and GPS'd within it, so quantification of accuracy was not possible, but just by comparing the classification to the digital camera imagery from the field, it appears that the model over-classifies forbs and green grass and under-classifies brush vegetation, including sage. Presumably, this is because there was more green growing vegetation within all classes, yet I developed the model to perceive the differences in vegetation that had already begun to mature or had already begun to senesce. Fields flown later in the season had an even higher percentage of senesced vegetation and tended to over-classify sage and dry grass and under classify green grass and forbs. This likely occurred because of the difference in flight dates. However, this time, there was more vegetation that had begun to dry out and senesce, making the spectral signatures brighter and more like dry types of vegetation.

The compositions of the fields flown were a mosaic of shrub, forb, and grasses. The classifications on field DB indicated a dispersed mosaic of all the classes, except for where a stream cut through the field. Field DB also had the most diversity, with four or more classes over 5% each of the total field size. Field DB had several dozen CSTG flushed by researchers walking through while inventorying ground control points. During plot inventories, Field T also had a dozen or more flushed CSTG. Fields H and T both had some distortions showing on the northern parts of the fields where it seemed there was an over-classification of forbs. This was presumably because of atmospheric conditions on those days; there was a lot of smoke from area wildfires. The accuracy of the individual classes was higher for all classes within the model, even throughout the growing season. The model was better at predicting the classifications in a binary system or one where presence or not of any one species is being measured. This could be important when looking for the occurrence of a single species within the season.

Overall, the classification worked to illustrate fine scale composition in the fields covered. It is important to remember that the leks for this area show an increase in the average count between 2001 and 2016. The ability to classify these areas and assess the success of the implemented CRP practices will be an important tool as managers continue to make recommendations to increase and rehabilitate CSTG numbers. The repeatability of classifications, with of the ability to deploy sUAS when and where needed, will aide managers in monitoring conservation practice efficacy and program compliance.

Chapter 5 Conclusion

Columbian Sharp-tailed Grouse are dependent upon large areas of contiguous shrub and grassland to establish lekking sites and subsequent nesting and brood locations. This research has shown that lek sites, and the number of individuals that visit those sites, are not necessarily influenced by their proximity to a change in landcover to agricultural production. Future work should focus on generating better bird count datasets and a more accurate classification of land cover from satellite imagery, as well as an investigation into the effect of land cover change due to fire on CSTG. This will be necessary to develop conservation practices that are more efficient in implementation to improve and promote habitat suitable for the species. The study area for the analysis of lek sites encompassed much of the area currently inhabited by CSTG within Idaho, so it is within these areas where the most focus should be placed for conservation practices. This research may also help to identify areas that may be the most influenced by conservation rehabilitation work and where the most efficient use of limited funds may be applied. Further research with a longer temporal period is warranted and will serve to analyze how land use changes, from agriculture to restored systems, affects the location and number of individuals frequenting lek sites.

The methodology implemented to map these fields can be implemented in future studies to generate fine scale vegetation classifications with an increase in temporal resolution. With increasing utilization of sUAS for ecological studies, the workflows presented herein will be applied to mapping and study at a fine scale level. It is recommended that the information and knowledge gained from this study will improve lek count numbers for these areas and for other leks in Southeast Idaho. Small unmanned aerial systems are a highly effective tool for natural resource researchers and managers, and many other disciplines for that matter. This study has supported others' works to show that the cost of deployment and richness of data acquired by sUAS makes them a great tool to be utilized by researchers and managers alike. Streamlining and refining of the workflows and processes employed by sUAS produces data products more quickly and efficiently than other comparable aerial or remote sensing platforms. As sensors continue to shrink, while at the same time improving in resolution and the amount of data captured, sUAS will become an invaluable part of wildlife and wildland research.

References

Adam, E., Mutanga, O., & Rugege, D. (2010). Multispectral and hyperspectral remote sensing for identification and mapping of wetland vegetation: A review. *Wetlands Ecology and Management*, *18*(3), 281–296. https://doi.org/10.1007/s11273-009-9169-z

Andersen, E., Gullett, B., Commons-Kemner, M., Knetter, J., Leptich, D., Lockyer, Z., … Sands, A. (2015). *Columbian Sharp-tailed Grouse Management Plan - 2015-2025*.

Berni, J. A. J., Zarco-Tejada, P. J., Suárez, L., González-Dugo, V., & Fereres, E. (2009). Remote sensing of vegetation from UAV platforms using lightweight multispectral and thermal imaging sensors. *Int. Arch. Photogramm. Remote Sens. Spatial Inform. Sci*, *38*, 6 pp. https://doi.org/10.1007/s11032-006-9022-5

Boisvert, J., Hoffman, R., & Reese, K. (2005). Home range and seasonal movements of Columbian sharp-tailed grouse associated with conservation reserve program and mine reclamation. *Western North American Naturalist*, *65*(1), 36–44.

Boon, M. A., Greenfield, R., & Tesfamichael, S. (2016). Unmanned Aerial Vehicle (UAV) photogrammetry produces accurate high-resolution orthophotos, point clouds and surface models for mapping wetlands. *South African Journal of Geomatics*, *5*(2), 186. https://doi.org/10.4314/sajg.v5i2.7

Buss, I. O., & Dziedzic, E. S. (1955). Relation of cultivation to the disappearance of the Columbian sharp-tailed grouse from southeastern Washington. *Condor*, *57*(3), 185–187.

Colomina, I., & Molina, P. (2014). Unmanned aerial systems for photogrammetry and remote sensing: A review. *ISPRS Journal of Photogrammetry and Remote Sensing*, *92*, 79–97. https://doi.org/10.1016/j.isprsjprs.2014.02.013

Connelly, J. W., Schroeder, M. A., Sands, A. R., & Braun, C. E. (2000). Habitat and management guidelines to manage sage grouse populations and their habitats. *Wildlife Society Bulletin*, *28*(4), 967–985. https://doi.org/10.2307/3783856

Costa, F. G., Ueyama, J., Braun, T., Pessin, G., Osorio, F. S., & Vargas, P. A. (2012). The use of unmanned aerial vehicles and wireless sensor network in agricultural applications. *2012 IEEE International Geoscience and Remote Sensing Symposium*, 5045–5048. https://doi.org/10.1109/IGARSS.2012.6352477

Cunliffe, A. M., Brazier, R. E., & Anderson, K. (2016). Ultra-fine grain landscape-scale quantification of dryland vegetation structure with drone-acquired structure-from-motion photogrammetry. *Remote Sensing of Environment*, *183*, 129–143. https://doi.org/10.1016/j.rse.2016.05.019

Falcucci, A., Maiorano, L., & Boitani, L. (2007). Changes in land-use/land-cover patterns in Italy and their implications for biodiversity conservation. *Landscape Ecology*, *22*(4), 617–631. https://doi.org/10.1007/s10980-006-9056-4

Getzin, S., Wiegand, K., & Schöning, I. (2012). Assessing biodiversity in forests using very high-resolution images and unmanned aerial vehicles. *Methods in Ecology and Evolution*, *3*(2), 397–404. https://doi.org/10.1111/j.2041-210X.2011.00158.x

Giesen, K. M., & Connelly, J. W. (1993). Guidelines for management of Columbian sharp-tailed grouse habitats. *Wildlife Society Bulletin*, *21*(3), 325–333. https://doi.org/10.1016/0006-3207(95)93787-D

Gonzalez, L. F., Montes, G. A., Puig, E., Johnson, S., Mengersen, K., & Gaston, K. J. (2016). Unmanned aerial vehicles (UAVs) and artificial intelligence revolutionizing wildlife monitoring and conservation. *Sensors (Switzerland)*, *16*(1). https://doi.org/10.3390/s16010097

Jensen, Austin M.; Baumann, Marc; Chen, Y. (2008). Low-cost mulitspectral aerial imaging using autonomous runway-free small flying wing vehicles. *IGARSS*, *5*, 506–509. https://doi.org/10.1109/IGARSS.2008.4780140

Jetz, W., Wilcove, D. S., & Dobson, A. P. (2007). Projected impacts of climate and land-use change on the global diversity of birds. *PLoS Biology*, *5*(6), 1211–1219. https://doi.org/10.1371/journal.pbio.0050157

Jones, G. P., Pearlstine, L. G., & Percival, H. F. (2006). An Assessment of Small Unmanned Aerial Vehicles for Wildlife Research. *Wildlife Society Bulletin*, *34*(3), 750–758.

Klott, J. H., & Lindzey, F. G. (1990). Brood Habitats of Sympatric Sage Grouse and Columbian Sharp-Tailed Grouse in Wyoming. *Journal of Wildlife Management*, *54*(1), 84–88.

Krauss, J., Bommarco, R., Guardiola, M., Heikkinen, R. K., Helm, A., Kuussaari, M., … Steffan-Dewenter, I. (2010). Habitat fragmentation causes immediate and time-delayed biodiversity loss at different trophic levels. *Ecology Letters*, *13*(5), 597–605. https://doi.org/10.1111/j.1461-0248.2010.01457.x

Laliberte, A. S., Winters, C., & Rango, A. (2011). UAS remote sensing missions for rangeland applications. *Geocarto International*, *26*(2), 141–156. https://doi.org/10.1080/10106049.2010.534557

Lambin, E. F., Turner, B. L., Geist, H. J., Agbola, S. B., Angelsen, A., Bruce, J. W., … Xu, J. (2001). The causes of land use and land cover change: Moving beyond the myths. *Global Environmental Change*, *11*(4), 261–269.

Leupin, E. (2003). *Recovery Strategy for: Columbian Sharp-tailed Grouse*.

Linchant, J., Lisein, J., Semeki, J., Lejeune, P., & Vermeulen, C. (2015). Are unmanned aircraft systems (UASs) the future of wildlife monitoring? A review of accomplishments and challenges. *Mammal Review*, *45*(4), 239–252. https://doi.org/10.1111/mam.12046

Liu, N., Budkewitsch, P., & Treitz, P. (2017). Examining spectral reflectance features related to Arctic percent vegetation cover: Implications for hyperspectral remote sensing of Arctic tundra. *Remote Sensing of Environment*, *192*, 58–72. https://doi.org/10.1016/j.rse.2017.02.002

Lucieer, A., Malenovský, Z., Veness, T., & Wallace, L. (2014). HyperUAS-Imaging Spectroscopy from a Multirotor Unmanned Aircraft System. *Journal of Field Robotics*, *31*(4), 571–590. https://doi.org/10.1002/rob.21508

Marks, J. S., & Marks, V. S. (1988). Winter Habitat use by Columbian Sharp-tailed Grouse in Western Idaho. *Journal of Wildlife Management*, *52*(4), 743–746.

Mayer, K. E. (2008). Greater sage-grouse population trends; an analysis of lek count databases 1965-2007. In *Canadian Consumer*. https://doi.org/10.1001/archopht.126.7.1012

McDonald, M. W., & Reese, K. P. (1998). Landscape Changes within the Historical Distribution of Columbian Sharp-tailed Grouse in Eastern Washington: Is There Hope? *Northwest Science*, *72*(1), 34–41. https://doi.org/10.1007/s13398-014-0173-7.2

Mozgeris, G., Jonikavičius, D., Jovarauskas, D., Zinkevičius, R., Petkevičius, S., & Steponavičius, D. (2018). Imaging from manned ultra-light and unmanned aerial vehicles for estimating properties of spring wheat. *Precision Agriculture*, *19*(5), 876–894. https://doi.org/10.1007/s11119-018-9562-9

Nackaerts, K., Everaerts, J., Michiels, B., Holmlund, C., & Saari, H. (2010). Evaluation of a lightweight UAS-prototype for hyperspectral imaging . *International Archives of Photogrammetry, Remote Sensing and Spatial Information Sciences*, *38*(5), 478–483. Retrieved from http://www.isprs.org/proceedings/XXXVIII/part5/papers/212.pdf

Ouerghemmi, W., Straigytė, L., Gadal, S., Mozgeris, G., Jonikavičius, D., & Juodkienė, V. (2018). Ultra-Light Aircraft-Based Hyperspectral and Colour-Infrared Imaging to Identify Deciduous Tree Species in an Urban Environment. *Remote Sensing*, *10*(10), 1668. https://doi.org/10.3390/rs10101668

Plieninger, T. (2006). Habitat loss, fragmentation, and alteration - Quantifying the impact of land-use changes on a Spanish dehesa landscape by use of aerial photography and GIS. *Landscape Ecology*, *21*(1), 91–105. https://doi.org/10.1007/s10980-005-8294-1

Rango, A., Laliberte, A., Herrick, J. E., Winters, C., Havstad, K., Steele, C., & Browning, D. (2009). Unmanned aerial vehicle-based remote sensing for rangeland assessment, monitoring, and management. *Journal of Applied Remote Sensing*, *3*(1), 1–15. https://doi.org/10.1117/1.3216822

Sardà-Palomera, F., Bota, G., Viñolo, C., Pallarés, O., Sazatornil, V., Brotons, L., … Sardà, F. (2012). Fine-scale bird monitoring from light unmanned aircraft systems. *Ibis*, *154*(1), 177–183. https://doi.org/10.1111/j.1474-919X.2011.01177.x

Skinner, W. R., & Majorowicz, J. A. (1999). Regional climatic warming and associated twentieth century land-cover changes in north-western North America. *Climate Research*, *12*(1), 39–52. https://doi.org/10.3354/cr012039

Storch, I. (2007). *Grouse: Status Survey and Conservation Action Plan 2006 –2010*. Retrieved from https://portals.iucn.org/library/sites/library/files/documents/2007-034.pdf

van Blyenburgh, P. (2013). 2013–2014 RPAS Yearbook: Remotely Piloted Aircraft Systems: The Global Perspective 2013/2014. *UVS International: Paris, France*.

Wright, C. K., & Wimberly, M. C. (2013). Recent land use change in the Western Corn Belt threatens grasslands and wetlands. *Proceedings of the National Academy of Sciences*, *110*(10), 4134–4139. https://doi.org/10.1073/pnas.1215404110

Xie, Y., Sha, Z., & Yu, M. (2008). Remote sensing imagery in vegetation mapping: a review. *Journal of Plant Ecology*, *1*(1), 9–23. https://doi.org/10.1093/jpe/rtm005

Zaugg, E., Edwards, M., & Margulis, A. (2010). Developing a small multi frequency synthetic aperture radar for UAS operation: The SlimSAR. *Proceedings of SPIE - The International Society for Optical Engineering*, *7669*. https://doi.org/10.1117/12.850207

Zhang, C., & Kovacs, J. M. (2012). The application of small unmanned aerial systems for precision agriculture: A review. *Precision Agriculture*, *13*(6), 693–712. https://doi.org/10.1007/s11119-012-9274-5